

## Review Article

# Stratification of the Low-Latitude and Near-Equatorial $F2$ Layer, Topside Ionization Ledge, and $F3$ Layer: What We Know about This? A Review

M. V. Klimenko,<sup>1</sup> B. Zhao,<sup>2,3</sup> A. T. Karpachev,<sup>4</sup> and V. V. Klimenko<sup>1</sup>

<sup>1</sup> West Department of Pushkov Institute of Terrestrial Magnetism, Ionosphere and Radio Wave Propagation RAS, Kaliningrad 236017, Russia

<sup>2</sup> Beijing National Observatory of Space Environment, Institute of Geology and Geophysics, Chinese Academy of Sciences, Beijing 100029, China

<sup>3</sup> State Key Laboratory of Space Weather, Chinese Academy of Sciences, Beijing 100190, China

<sup>4</sup> Pushkov Institute of Terrestrial Magnetism, Ionosphere and Radio Wave Propagation RAS, Troitsk 142190, Russia

Correspondence should be addressed to B. Zhao, zbjz@mail.iggcas.ac.cn

Received 14 November 2011; Accepted 6 February 2012

Academic Editor: R. Dabas

Copyright © 2012 M. V. Klimenko et al. This is an open access article distributed under the Creative Commons Attribution License, which permits unrestricted use, distribution, and reproduction in any medium, provided the original work is properly cited.

A large number of researches have been devoted to the formation of additional layers in the  $F$  region of the equatorial ionosphere, first of which has been published in 1940s. Originally the occurrence of such layer was named “stratification of equatorial  $F2$  layer.” The additional layer was later named as the  $F3$  layer. The theoretical researches have shown that the  $F3$  layer is formed by zonal component of electric field with assistance of meridional component of thermospheric wind and field-aligned plasma diffusion. The physical mechanism of the  $F3$  layer formation is clearly formulated for the morning-noon period, although the  $F3$  layer is also observed at other hours. This paper presents a brief review into the history of the additional layer researches, describes the current progress of these researches, and identifies the most important problems in this field of the ionospheric physics.

## 1. Early Study of the Stratification of the $F2$ Layer

**1.1. Ground Observation.** The earliest revelation of multilayer structure in the  $F2$  region over the equatorial ionosphere can be traced back to the middle of the last century. Bailey [1] briefly reported that for ionospheric stations situated near the minimum of the equatorial ionization trough a very significant feature of the  $h'F$ -curves during the daytime is the remarkable tendency to be subdivided into two and sometimes more layers. In the South Asian region, Sen [2] presented some multilayer cases in January and February over Singapore (geographic latitude  $1.3^\circ\text{N}$ , geographic longitude  $103.7^\circ\text{E}$ ; magnetic latitude  $-9.2^\circ$ ). The ionospheric measurements indicated that the  $F2$  layer was daily stratified into three discrete layers during the daylight hours (Figure 1). This is rather an interesting feature because

the duration of the multistratification lasts for 10 hours while such cases were seldom reported in the present study. Osborne [3] also presented some ionograms of two-layer stratification in the  $F2$  region at Singapore and pointed out that the complex  $F2$  structure cannot be described adequately using the conventional and internationally recognized symbols and terminology.

In the South American region, Ratcliffe [4] observed an addition layer in  $h'F$  records from Huancayo ( $12.1^\circ\text{S}$ ,  $75.3^\circ\text{W}$ ;  $1.2^\circ$ ), Peru, at sunspot minima 1944. The measurements show that the high frequency end of the  $h'F$  ionogram records a “spur” which moves to higher frequencies during the morning-noon sector. McNish [5] represented an upward-moving layer (the “spur”) at Huancayo based on the measurement in 1939. Similar results were presented by Osborne [6] on the basis of the measurement during 1948–1951 at Singapore. In the African region, more characteristics

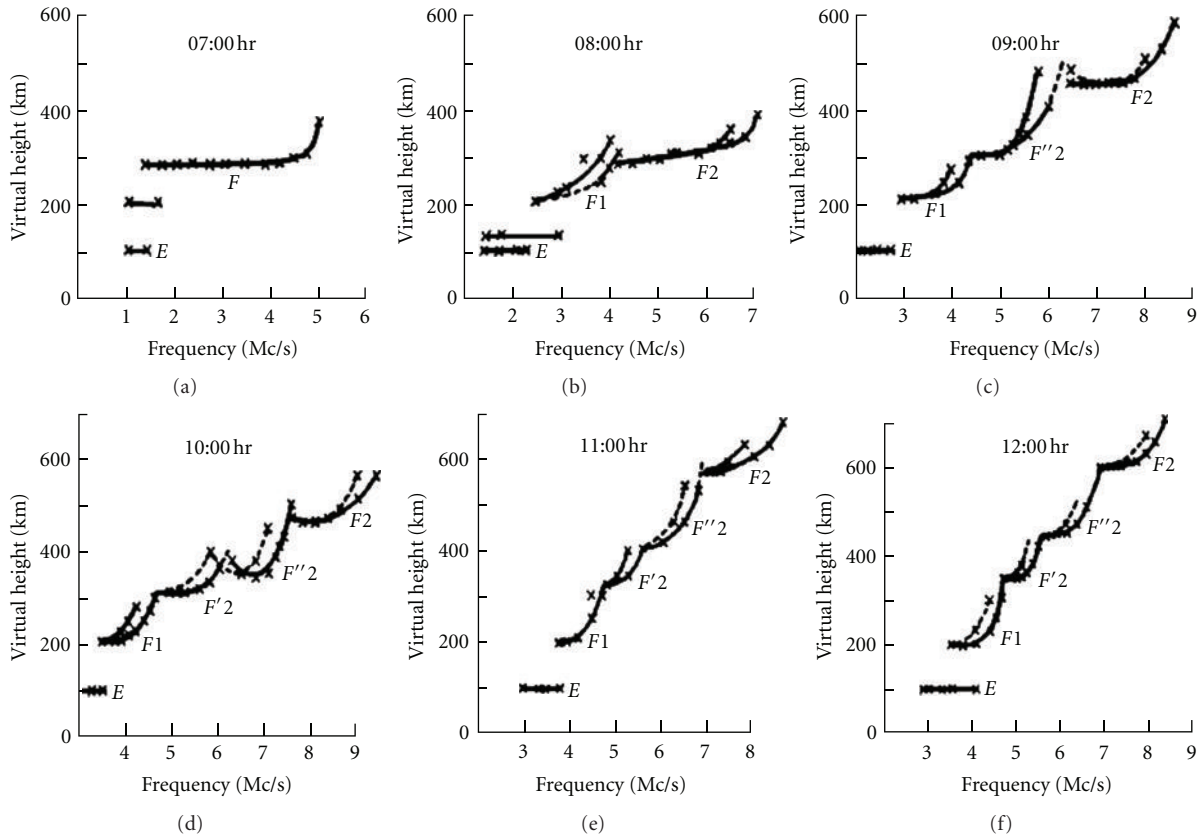


FIGURE 1: Typical curves of virtual height against frequency, January 8, 1946 (from Sen [2]).

about the occurrence of stratification of  $F_2$  layer (“ridge”) have been revealed by Skinner et al. [7] according to the observation at Ibadan ( $7.4^\circ\text{N}$ ,  $3.9^\circ\text{E}$ ;  $-2.1^\circ$ ), Nigeria during 1951–1953. They found that there are more morning ridges in winter than in summer and also there is a correlation between the maxima in the lunar tide of morning ridge occurrence and the minima in the lunar tide of noon  $foF_2$ .

Also the existence of additional layers above the regular  $F_2$  layer was presented in some papers such as in Heisler [8], Faynot et al. [9], Rastogi [10], and Sario et al. [11]. These experimental evidences were based on the observational data both of ground ionospheric sounding and incoherent scatter radars. At the equator the bifurcation (stratification) of the  $F_2$  layer begins to occur at about 12:00 LT and ends at about 19:00 LT according to McClure and Peterson [12] based on the result of the observations made with Thomson scatter radar. Woodman et al. [13] reported a bifurcation of the  $F_2$  layer which was observed on a magnetic storm day, 8 March 1970.

According to Huang [14] the value of  $foF_2$  obtained from the vertical sounding is qualified with a letter H if a stratification of  $F_2$  layer exists. The monthly tables of  $foF_2$  observed at a sequence of stations along  $75^\circ\text{W}$  meridians were examined, and it was found that the occurrence of the stratification was quite regular at Chimbote ( $3.9^\circ\text{S}$ ,  $78.6^\circ\text{W}$ ;  $2.2^\circ$ ), Peru, in March 1958, as it is shown in Figure 2. The occurrence of stratification was much less at Bogota ( $4.6^\circ\text{N}$ ,

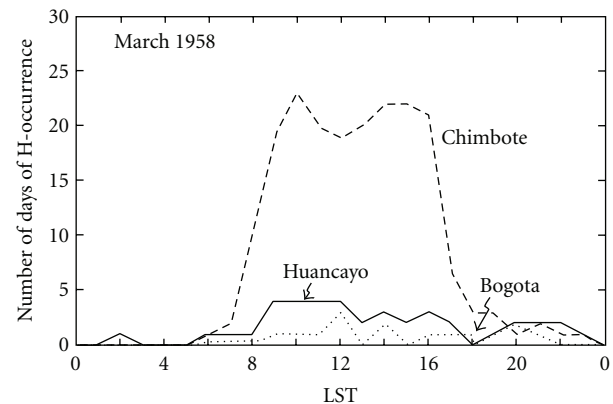


FIGURE 2: The number of days on which the stratification of the  $F_2$  layer has been observed (from Huang [14]).

$74.1^\circ\text{W}$ ;  $16.0^\circ$ ), Colombia, as was expected from Huang’s computation [14]. However, the occurrence of the  $F_2$  layer stratification was unexpectedly low at Huancayo ( $12.1^\circ\text{S}$ ,  $75.3^\circ\text{W}$ ;  $-0.6^\circ$ ). In order to obtain an exact picture of the bifurcation near the equator, it may be useful to reexamine the ionograms.

Huang [15] plotted the percentage occurrence of the bifurcation for July 1957–December 1958 (see Figure 3).

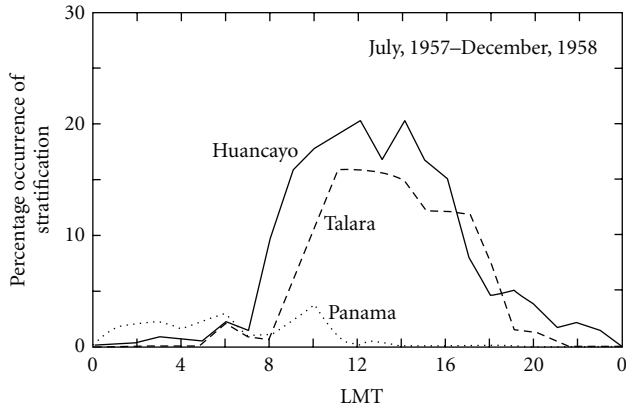


FIGURE 3: Diurnal variation of percentage occurrence of the  $F_2$  layer stratification during the IGY period (from Huang [15]).

The occurrence of the  $F_2$  layer stratification is high from 08:00 LT to 17:00 LT at Huancayo and 1-2 hours later at Talara ( $4.6^\circ\text{S}$ ,  $81.2^\circ\text{W}$ ;  $6.6^\circ$ ), Peru. At Panama ( $9.4^\circ\text{N}$ ,  $79.9^\circ\text{W}$ ;  $20.6^\circ$ ), the diurnal pattern is completely different, the high occurrence being during 01:00–11:00 LT. From the latitudinal viewpoint, the occurrence is the highest at Huancayo ( $-0.6^\circ$ ), a few percent lower at Talara ( $6.6^\circ$ ), and very low at Panama ( $20.6^\circ$ ). All of these features suggest that the same conditions which lead to the bifurcation may also be the conditions for H-occurrence in the equatorial belt. However, the correspondence of H-occurrence at Huancayo and at Talara is poor, even if the time lag is considered. The seasonal variation is not only indistinct but also inconsistent for the two stations, and therefore the statistics used by Huang [14] for March 1958 are different from those in Huang [15].

**1.2. Satellite Observation.** The spatial distribution of stratification of the  $F_2$  layer can be observed by the satellite equipment. However, the satellite observations have some limitations: it is difficult to remove the problem with the equipment, interruptions in its work, the lack of onboard memory, poor quality of nighttime ionograms due to the strong  $F$  spread, and so forth. In addition, there are limited satellites probing the outer ionosphere: Alouette 1 and 2, ISIS-1 and 2, ISS-b, EXOS-C (Ohzora), Intercosmos-19, and Cosmos-1809. As a result, the satellite studies of the equatorial  $F_2$  layer stratifications are scarce. Alouette, ISIS, and EXOS-C satellites data are almost entirely for low solar activity and limited to the American, Indian, and Pacific longitudinal sectors such as the ground-based measurements. Therefore the diurnal ionospheric variations measured by these satellites are described incompletely. Only IK-19 and ISS-b are satellites that supplied the topside sounding data for all longitudes, local times, and seasons. The investigation of stratification of the  $F_2$  layer occurrence was not performed in general with use of topside sounder data onboard the ISS-b satellite for moderate solar activity [16]. The IK-19 is the only satellite that supplied the topside sounding data during high solar activity (1979–1981) for all longitudes,

local times, and seasons. However, to the present time it has been published only two IK-19 satellite studies devoted to the additional layers. All of these studies were focused on specific cases.

Sayers et al. [17] were the first to detect the topside ledges in the equatorial ionosphere using a Langmuir probe onboard the Ariel-I satellite, and they predicted that the topside ionograms would reveal the ledges as cusps. Lockwood and Nelms [18] and King et al. [19] detected the ledges as cusps in the topside ionograms recorded by the topside sounder onboard the Alouette-I satellite. Figure 4 shows an example of Alouette-1 low-latitude topside ionogram from [18]. The distinctive feature of this ionogram is a cusp on both O-mode and X-mode echoes at frequencies of 2.5 MHz. Usually the cusp appears on ionograms from about geomagnetic latitudes  $\pm 15^\circ$  at frequencies close to  $foF_2$ , and then its frequency decreases when approaching the geomagnetic equator. At geomagnetic latitudes of  $\pm 15^\circ$ , the ledge merges with  $F$  layer peak, and approaching the equator, its height grows up to heights of 1000–1200 km [18]. Figure 5 shows a typical examples of the ledges on a real height topside  $N(h)$  distribution and an equatorial backscatter distribution [19]. It is evident that both techniques show the same phenomenon—ledge, that is, a local enhancement in electron density profiles at height above the regular  $F_2$  layer.

Raghavarao and Sivaraman [20] detected the afternoon ledges in the Indian longitudes using the ISIS-II topside sounder data collected at Ahmedabad ( $32.1^\circ\text{N}$ ,  $44.3^\circ\text{E}$ ;  $26.9^\circ$ ). The maximum percentage deviations of the ledge electron density were observed to increase toward the magnetic equator reaching a maximum value of 16%. Raghavarao et al. [21] considered longitudinal dependence of the ionization ledges. The ledges are seen to occur with different intensity at two close by longitudes. These features of the ionization ledges are identical to those exhibited by the equatorial counter electrojet (CEJ) phenomenon. Sharma and Raghavarao [22] have analyzed 577 good daytime passes of ISIS-1 and ISIS-2 satellites collected at Ahmedabad, recorded during the period February 1972–March 1975 and detected the occurrence of the ionization ledges on 216 days reaching 37%. Based on data for 168 quiet days of 1972–1974, 70% correlation was obtained for the simultaneous occurrence of the ledge and the CEJ [22].

King et al. [19] and Lockwood and Nelms [18] showed that both the peak of the ionization ledges and the equatorial ionization anomaly (EIA) crests are aligned along the same field line. Lockwood and Nelms [18] examined the Alouette-1 data for 3 months in 1962 to cover the period from 06:00 to 24:00 LT. They have found that the equatorial ionosphere in the minimum of solar activity at all altitudes has the form of the dome from sunrise until 17:00 LT. Figure 6 shows the height-latitude section of the equatorial ionosphere, obtained for the October 21, 1962. The ionization ledge lying along the magnetic field line passing through the EIA crests. The apex of this magnetic field line rises from around 670 km at 18:10 LT to around 780 km at 19:42 LT. The same results were obtained by Raghavarao and Sivaraman [20] with use of ISIS-2 satellite data. However, Sharma and Raghavarao [22] observed that until about 16:00 LT, both the peak of

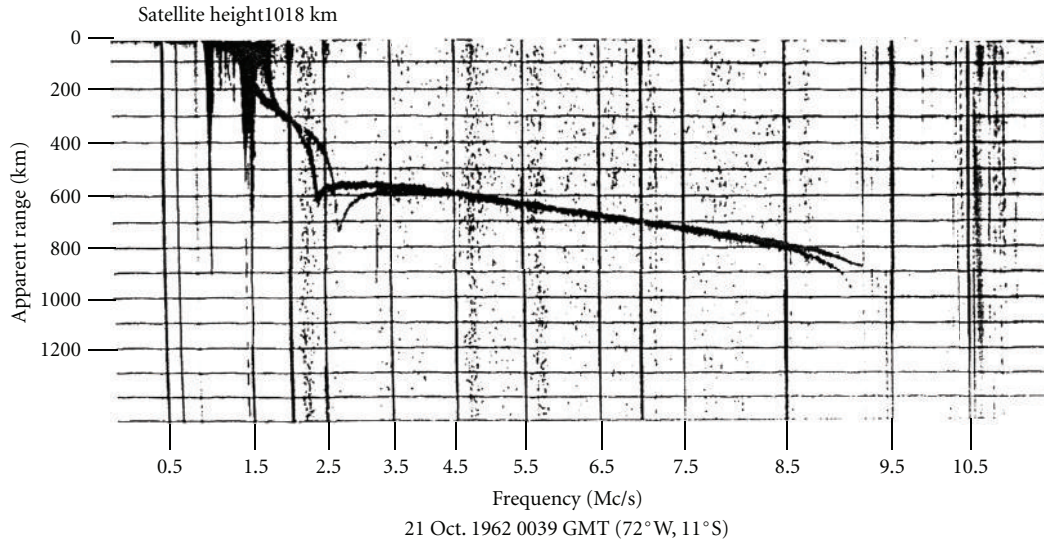


FIGURE 4: Ionogram recorded by topside sounding onboard Alouette-1 satellite that provides an evident cusp example (from Lockwood and Nelms [18]).

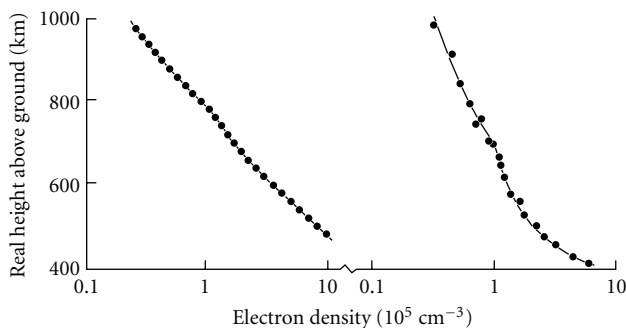


FIGURE 5: Electron density distributions showing the field-aligned ledge (from King et al. [19]). Both the topside sounder and incoherent backscatter techniques show the same phenomenon. Left, Alouette-1 satellite data over Singapore, revolution 290, 15th profile. Right, Jicamarca, Peru, ISR data 24 April 1962, 06:10 EST.

the ionization ledge and the EIA crest were located along the same geomagnetic field line (with apex at height of  $\sim 850$  km) and were separated afterwards. Prutensky [23] using Cosmos-1809 satellite data on 5 June 1987 revealed that the ledges are located over the equator in the shape of a dome, but not along the geomagnetic field line (Figure 7). It is also evident that the bottom limits of the ledge are horizontal. Note the EIA is weakly developed at this case. Thus, the problem of the ledge location about the crests of EIA and the geomagnetic field line cannot be regarded as solved.

**1.3. Theoretical Results.** The equatorial ionosphere has been studied theoretically for a long time. Martyn [24] proposed a mechanism explaining the EIA formation (the so-called “fountain effect”). McNish [5] first reported that the phenomenon of the “spur” at Huancayo was related to lunar time that indicates the relationship between the “spur” and the

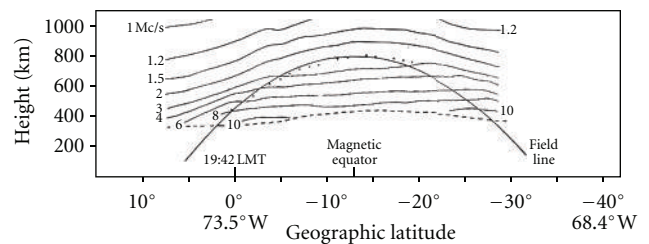


FIGURE 6: Contours of constant electron density at 19:42 LT. Points show the height of the ledge according to one Alouette-1 satellite path (from Lockwood and Nelms [18]). The dashed line is the height of the  $F_2$  layer peak.

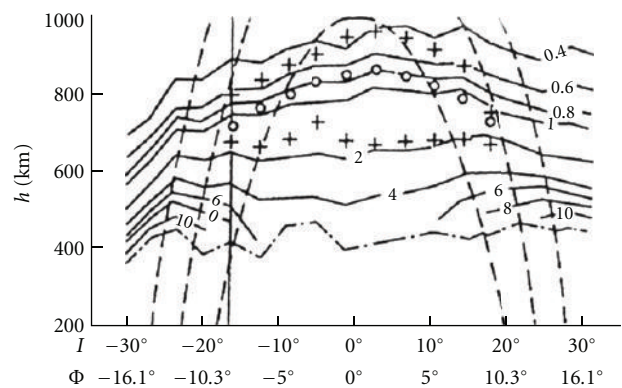


FIGURE 7: Isolines of the electron density (solid lines) in  $10^6 \text{ cm}^{-3}$ , plotted according to the data of outer sensing of the ionosphere at the turn of 2333 June 5, 1987. Dash-dotted line shows  $h_m F_2$ , dashed lines: the geomagnetic field lines with tops at 1000, 1500, and 2000 km, the vertical line marks the position of the geographic equator, crosses show the upper and lower limits of the stratification, triangles: the upper limit of the stratification above the satellite altitude, circles: position of the maximum of ionization ledge. (from Prutensky, [23].)

thermospheric tides. Similar presentation of lunar control of the times of appearance of ledges in the upper  $F2$  region was presented by Osborne [6] at Singapore. The field-aligned enhancements in the neutral densities (neutral anomaly) inhibit the plasma flow along the field lines and thus are primarily responsible for the enhancement of ionization along a particular field line. It was conjectured that, because of the enhanced  $O$  concentration along this field line, the diffusion coefficient and therefore the diffusion parallel to the field line would be decreased by about 10%, resulting in some sort of an accumulation of ionization [20]. Sharma and Raghavarao [22] proposed that the ledge and the CEJ are caused by a common agency, which is the neutral anomaly at heights of the  $F$  region. Vasiliev [25] suggested that with increase of distance from equator, the role of internal gravity waves in the formation of the equatorial  $F2$  layer stratifications increases. This hypothesis is used at present to explain the formation of the stratifications at the latitudes of the EIA crests in quiet geomagnetic conditions [26].

The researchers that observed an additional layer above the  $F2$  layer maximum noted that it was necessary to perform studies using the numerical model, taking into account the electromagnetic drift and the effects of transequatorial thermospheric winds, in order to understand this specific feature. Anderson [27] proposed an original and effective approach to the solution of three-dimensional hydrodynamic equations for ionospheric plasma as applied to the equatorial ionosphere (the so-called pseudo-Lagrangian approach, which takes into account the property of thermal plasma magnetization in the ionospheric  $F$  region) and started theoretically studying the equatorial ionosphere based on numerical models. This approach makes it possible to separate diffusion motions of plasma under the action of pressure gradients along geomagnetic field lines and electromagnetic drift motions of plasma tubes.

Huang [14, 15] was the first to demonstrate that the simple numerical models could reproduce stratification of equatorial  $F2$  layer. In these studies it was suggested connection of the equatorial  $F2$  layer stratifications with the formation of the equatorial anomaly. Huang [14] demonstrated the importance of nocturnal ionization in the  $F2$  layer stratification process (Figure 8). The travelling bifurcation revealed by the computation made by Huang [14] was also found in the vertical sounding data of the IGY period more often during 10:00–14:00 LT. Huang [15] suggested the physical mechanisms that lead to the formation of a bifurcated  $F2$  layer during noon and afternoon hours. When the diffusion is small, the ionization of the  $F2$  layer peak which is lifted rapidly according to the vertical plasma drift at the equator is transported to higher latitudes slowly. After the vertical plasma drift begins to decrease at 10:00 LT, the photoionization produced at a lower height accumulates and develops into a new stratification, and thus forms a bifurcated  $F2$  layer. On the other hand, if the diffusion is large, the upper part of the original  $F2$  layer loses its electrons quickly, and the lower part is combined with the ionization accumulated at a lower height to form a single layer. A high value of upward drift favors the formation

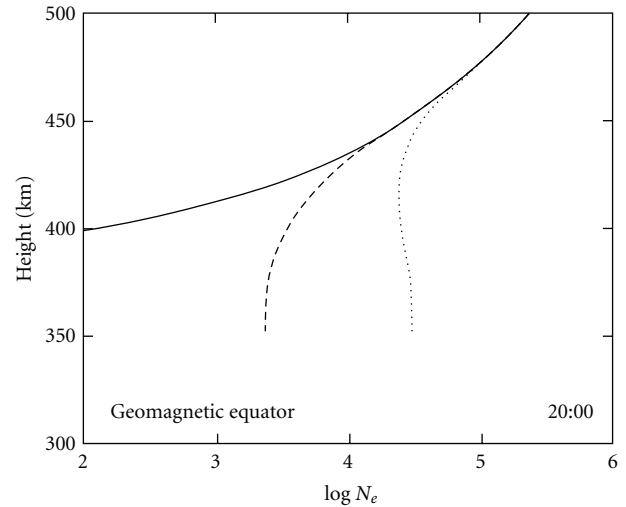


FIGURE 8: The height distribution of  $\log N_e$  at 20:00 LT on the equator. The full, dashed, and dotted lines represent the cases in which the nocturnal ionization productions are 0%, 0.2%, and 2% of noon production respectively (from Huang [14]).

of bifurcation, but the values of the effective attachment coefficient and ion production rate scarcely affect it. The bifurcated structure travels to higher latitudes for a smaller diffusion coefficient. The bifurcation observed at sunrise, which has not been revealed by the computation, seems to be formed by a somewhat different mechanism. The vertical sounding data indicate that the high layer peak continues for a few hours before a new stratification due to the rapid increase of photoionization is developed at a lower height. So Huang [15] found that the formation of the  $F2$  layer bifurcation is principally due to the combined effect of the upward drift, which changes from increasing to decreasing at 10:00 LT, and the slow diffusion.

Numerical studies of the stratification of equatorial  $F2$  layer were subsequently continued by [28]. Surotkin et al. [28] as early Raghavarao and Sivaraman [20] suggested that the stratification of equatorial  $F2$  layer in the morning and noon hours is formed due to the inhomogeneity “fountain effect” across the geomagnetic field. So, an excess of plasma rises upward by an electric field above the equator and drops to the crest of the EIA by the diffusion flux that changes non-monotonically across the geomagnetic field. The latitudinal gradients in the electron density in the crests of the EIA, the nonstationary of electromagnetic drift, and ionization lead to this non-monotone diffusion flux. The disadvantage of this hypothesis is that its authors take into account the  $\mathbf{E} \times \mathbf{B}$  plasma drift only at the geomagnetic equator, while the equatorial anomaly crests remain motionless. In reality, the  $\mathbf{E} \times \mathbf{B}$  drift acts to the plasma tube as a whole.

Surotkin et al. [29] discussed the formation mechanisms of the stratifications of the equatorial  $F2$  layer during quiet geomagnetic condition. Surotkin et al. [29] as Huang [15] noted that the zonal plasma drift is the most essential process in the occurrence of stratifications in the morning. In addition, these papers demonstrated that, in general, the model

simulations reproduced the stratifications of the equatorial  $F_2$ -layer when the zonal electric field is included to the model run. Surotkin et al. [29] noted that the possible factors assisting the occurrence of stratifications in the morning are (1) displacement of maximum of upward  $\mathbf{E} \times \mathbf{B}$  drift related to the action of zonal electric field in the morning sector; (2) the presence in the afternoon sector of the meridional electric field directed upwards at the equator, causing the zonal plasma drift from the day side to dawn side; (3) the phase delay of daily variation of the zonal electric field at geomagnetic equator with regard to the variation of electric field at nearby latitudes. So they for the first time showed the influence of the latitudinal dependence of the zonal electric field onto the appearance time of the equatorial  $F_2$  layer stratifications. The zonal plasma drift was found to be the most essential process in the formation of stratifications in the morning. Kashchenko and Nikitin [30] showed that short-lived daytime  $F_2$  layer stratifications appear in a narrow equatorial band with width of  $\sim 15^\circ$  at the weakening of the upward drift due to the formation of a new peak at lower altitudes. They showed that the latitudinal extent and lifetime of this phenomenon depend on the rate of decay of the eastward component of the electric field (the vertical drift nonstationarity), the velocity of diffusion along geomagnetic field lines, and the character of the wind drag. Surotkin et al. [31] have shown that the appearance of the  $F_2$  layer stratifications occurs when the maximum of electron density is lifted upward into the region of predominance of the diffusion processes. Surotkin et al. [31] showed that the physical cause of the formation of  $F_2$  layer stratifications is nonuniform diffusive plasma outflow from the region over the magnetic equator at the equatorial anomaly crests developed. In the plasma tubes of the geomagnetic field lines with the equatorial anomaly crests, the diffusive plasma outflow from the region above the equator slows. This leads to a relative accumulation of plasma over the equator at altitudes above the maximum of  $F_2$  layer, which leads to an additional maximum. Figure 9 illustrates the formation of the nonuniform plasma diffusion in the height region above the geomagnetic equator. In addition, Surotkin et al. [31] showed that large-scale irregularities could decay into small-scale irregularities. Unfortunately, the papers [28–31] were published in the Russian literature and are largely unknown to the foreign ionosphere research community. Note that authors of all these works are talking about the formation mechanisms of  $F_2$  layer stratification at the equatorial ionosphere, that is, about not only the formation of an additional maximum in the vertical profile of electron density above or below the maximum of  $F_2$  layer, but also the formation of a minimum between two maxima.

## 2. Progress of the Recent Study on the Stratification of the $F_2$ Layer ( $F_3$ Layer)

So the studies of the stratification of the  $F_2$  layer gradually subsided after 1970s until recent theoretical works based on the Sheffield University Plasmasphere-Ionosphere Model (SUPIM). Balan and Bailey [32] suggested that the equatorial

plasma fountain and the plasma flow outside the fountain could produce a temporary additional layer (“ $G$ ” layer) above the normal  $F_2$  peak. At the equator, the maximum plasma concentration of the  $G$  layer can be greater than that of the  $F$  layer for a short period of time just before noon (when the  $\mathbf{E} \times \mathbf{B}$  drift starts to decrease). The  $G$  layer has a geomagnetic latitudinal coverage of about  $\pm 10^\circ$  and local time coverage over 10 hours (from 10:00 to 22:00 LT) at the magnetic equator. This additional layer was later renamed as the  $F_3$  layer due to the same chemical composition as the  $F$  region [33]. It is obvious that the equatorial  $F_2$  layer stratification and the occurrence of an additional layer in the equatorial ionosphere is the one phenomenon.

*2.1. Methods of the Investigation.* After Balan and Bailey [32], the subject of the  $F_3$  layer received extensive investigations at low and equatorial latitudes concerning its spatial and temporal distribution based on the ionosonde observations of single or several stations distributed at three longitudinal sectors (American, Indian, and Pacific longitudes) [34–44]. From these investigations, it is known that the  $F_3$  layer can be observed under geomagnetically quiet conditions. The critical frequency of  $F_3$  layer becomes greater than that of the  $F_2$  layer within about  $\pm 10^\circ$  magnetic latitudes during morning-noon period (08:00–16:00 LT). The  $F_3$  layer appears with higher occurrence and lasts longer on the summer side of the geomagnetic equator during low solar activity periods. In addition to being seen either at the magnetic equator or in the low-latitude summer hemisphere, the  $F_3$  layer can also be seen in both regions simultaneously.

Note that ground-based ionosonde may detect the  $F_3$  layer only when its peak density can become greater than that of the  $F_2$  layer. The example of such observations is presented in Figure 10, which displays some sample ionograms recorded at Fortaleza ( $4.0^\circ\text{S}$ ,  $38.0^\circ\text{W}$ ;  $-9.0^\circ$ ), Brazil, from Balan et al. [33]. All sharp increases in height of  $F$  maximum peak, both in quiet and in the storm-time conditions, are connected as was shown by Klimenko et al. [45, 46] and M. V. Klimenko and V. V. Klimenko [47, 48], with the appearance of the additional layers ( $F_3$  and  $F_4$ ) formed in the vicinity of geomagnetic equator at heights larger than the  $F_2$  layer maximum. When the critical frequency of additional layers,  $foF_3$  ( $foF_4$ ), becomes greater than  $foF_2$  ( $foF_3$ ), the jump in  $F$  layer maximum height occurs. Sharp decreases in  $h_mF$  are connected with transition from the case when  $foF_3$  ( $foF_4$ )  $>$   $foF_2$  ( $foF_3$ ) to the case when  $foF_3$  ( $foF_4$ )  $<$   $foF_2$  ( $foF_3$ ).

As shown in Section 1.2, the low-latitude ionosphere is also known to contain topside ledges. Uemoto et al. [49, 50] reported that the ledges observed in the noontime period are qualitatively similar to the  $F_3$  layer predictions by Balan and Bailey [32], and the ledge tends to move upward during morning-noon period. Below we will use both terms (the ledge and  $F_3$  layer) believing that we are dealing with the same physical phenomenon—a stratification of the equatorial  $F_2$  layer. In addition to satellite studies presented in Section 1.2, the ionization ledges were also observed by using the topside sounders onboard the Ohzora (EXOS-C)

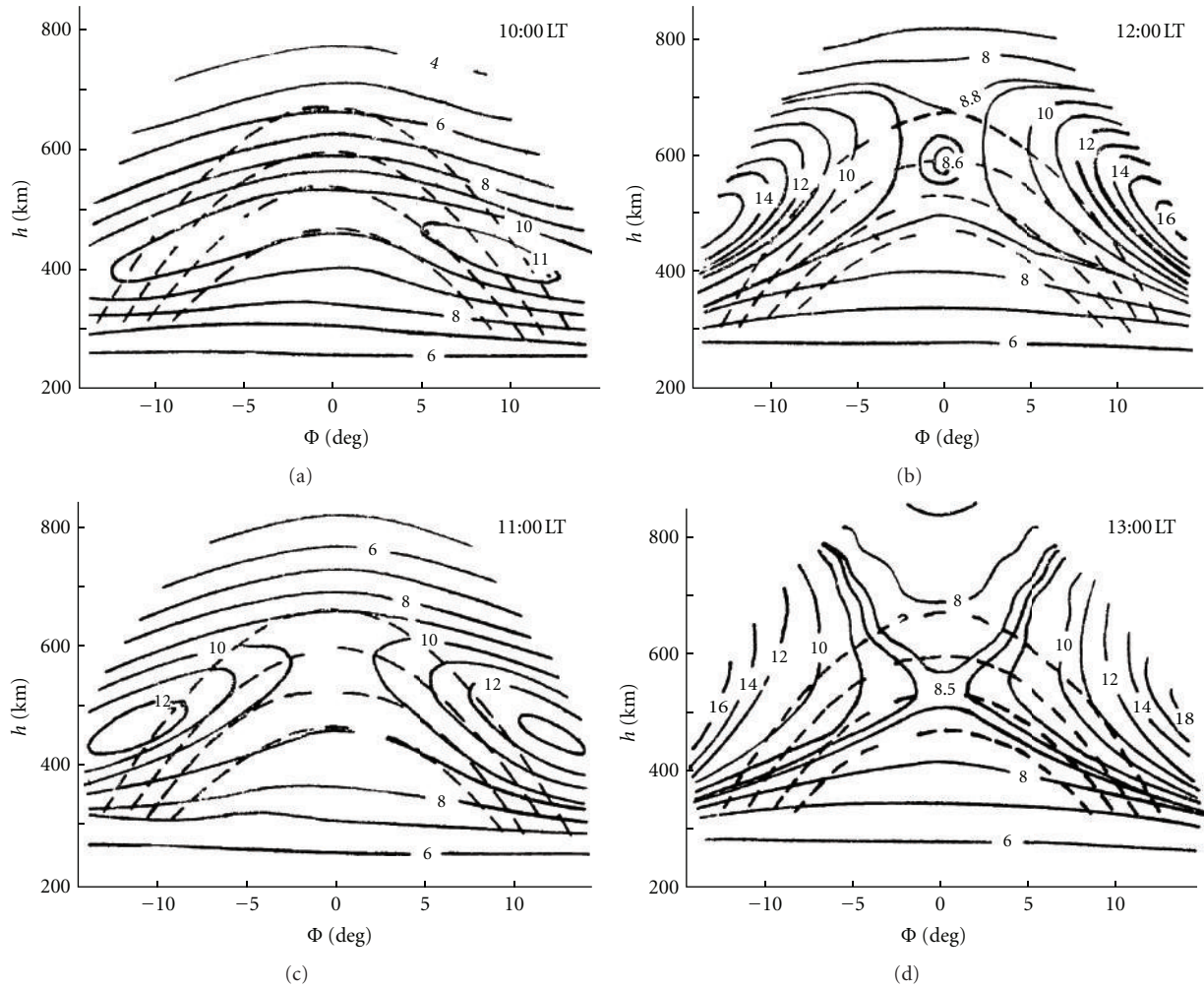


FIGURE 9: Latitudinal profiles of the plasma frequency isolines at 10:00, 11:00, 12:00, 13:00 LT for the geomagnetic latitude of station Jicarmarca, calculated using a numerical model of the equatorial ionosphere (from Surotkin et al. [31]). The dashed lines show the geomagnetic field lines.

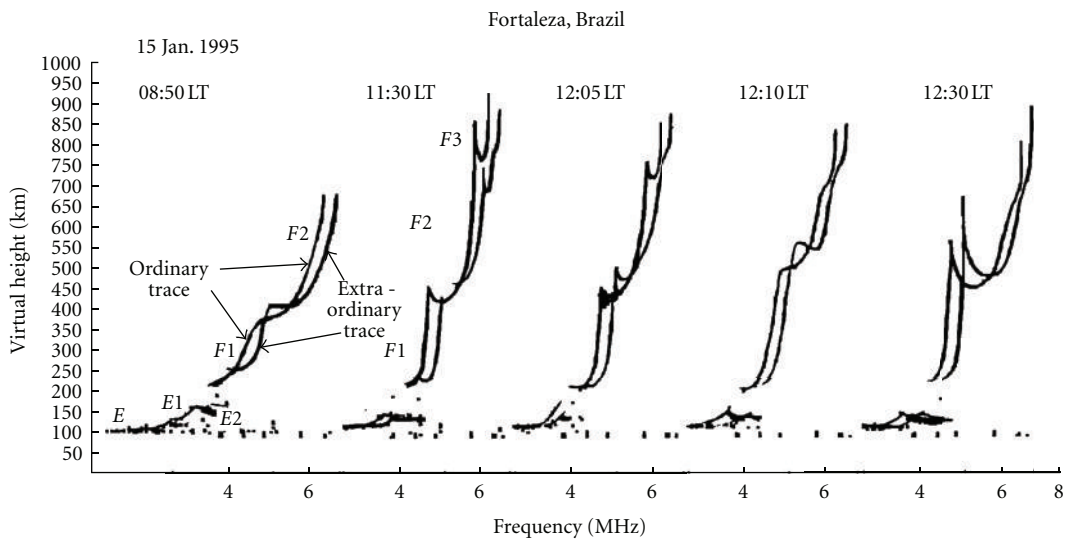


FIGURE 10: Sample ionograms recorded at Fortaleza on January 15, 1995. Note the development and decay of the F3 layer as an additional trace at the high-frequency end at the virtual altitude of about 750 km, which is most distinct at 11:30 LT (from Balan et al. [33]).

satellite by Uemoto et al. [49, 50], and Intercosmos-19 (IK-19) satellite by Depuev and Pulnits [51], and Karpachev et al. [52]. Figure 11 shows a typical example of IK-19 low-latitude topside ionograms for early morning and daytime conditions. The distinctive features of these ionograms are the cusps on both *O*-mode and *X*-mode echoes. Cusps can be pronounced or not very noticeable. Since the high frequency part of the *O*-mode echo is absent,  $foF2$  can be defined by reflection from the Earth's surface. Note that the reflections from the Earth are often absent. This is a typical feature of the equatorial ionograms during daytime. This feature makes the interpretation of ionograms and statistical analysis of the *F3* layer characteristics complicated.

The cusp is a sign of a ledge, that is, a local enhancement in electron density profiles at height above the regular *F2* layer [18, 19]. Figure 12 shows an example of the ledge observation from the Ohzora (EXOS-C) satellite [49]. The ledge with the plasma density increases with about 24% above the smoothed plasma density profile was observed from the ISIS-2 satellite [50]. Lockwood and Nelms [18] demonstrated a 10% increase in topside electron density at the occurrence of ionization ledge. Sharma and Raghavarao [22] demonstrated a 13–17% increase in topside electron density, Uemoto et al. [50] indicated an ~60% increase in the daytime from the ISIS-2 data for low solar activity, and recently Karpachev et al. [52] show the topside electron density increases by 10–15% during daytime and by 30% at night. Karpachev et al. [52] studied the equatorial ionization ledge based on large dataset (about 3600 passes across the equator) of high spatial resolution IK-19 topside sounding. Figure 13 shows the examples of three IK-19 latitudinal distributions of electron density with EIA observed during different local time and geomagnetic conditions [52].

Thampi et al. [53] were the first to show that the additional layers in the low-latitude ionosphere could be observed in the total electron content (*TEC*) measured at Trivandrum (8.5°N, 76.9°E, 0.5°), India. The ionization ledges were shown to have their clear signatures in the latitudinal profiles of the relative *TEC* derived using the differential Doppler measurements made at a single station. Thampi et al. [54] through this method provided the first observational evidence that the so-called “humps” in the latitudinal variation of *TEC* are the upward propagating *F3* layer. Recently, Zhao et al. [55] presented a statistical work to infer the *F3* layer spatial structure at low latitude area using the electron density profiles derived from radio occultation (RO) technique of COSMIC/FORMOSAT3 (see Figure 14). However, it is known that the accuracy of COSMIC electron density profiles retrieval depends on several assumptions, where the most significant one is the spherical symmetry of electron density hypothesis. The large horizontal gradients in the ionospheric electron density at low and equatorial areas can produce a false stratification. To exclude this situation, Zhao et al. [55] choose a scale for the track of occultation. The *F3* layer in electron density profile was recognized through the altitude differential profile featured by two maxima existing from 220 km to the peak height of the electron density. Only the most clear-cut cases of the *F3* layer occurrence when its maximum was greater than the *F2*

layer maximum were selected from COSMIC observation to avoid the errors [55]. But this actually means that from the entire database of COSMIC observation they selected only the same cases of the *F3* layer occurrence that are detected from ground-based sounders. Thus, all cases when the *F3* layer existed and  $foF3 < foF2$  were not considered. Note the *F3* layer cases that satisfy all Zhao et al. [55] criteria account for 2.07% of the total number of profiles (~448,000 occultation events), which is much lower than the occurrence at a single ionosonde site. The low percentage of the COSMIC-derived *F3* is due to the strict restrictions on the choice of the RO event and *F3* identification in order to avoid the large horizontal gradients and retrieval errors in the ionospheric electron density.

Many theoretical works with respect to additional layer formation were based on the SUPIM model [33–35, 38, 54, 56, 57]. Lin et al. [58, 59] run the SUPIM model, using the thermosphere-ionosphere general-circulation model (TIEGCM) [60, 61] simulated neutral winds, temperature, and composition as inputs during strong geomagnetic storm. Recently M. V. Klimenko and V. V. Klimenko [47, 48] and Klimenko et al. [45, 46] showed that the global self-consistent model of the thermosphere, ionosphere and Protonosphere (GSM TIP) [62, 63] reproduces the *F2* layer stratification and the *F3* layer occurrence in the near-equatorial region. It was concluded that to reproduce the dynamo electric field and thereby the *F3* layer during quiet geomagnetic conditions it is necessary to take into account the thermospheric tides in the model runs [47, 48]. To reproduce the *F3* layer occurrence during geomagnetic storms, it is necessary to take into account both the dynamo electric field and the penetration of the magnetospheric convection electric field to lower latitudes [45, 46]. Uemoto et al. [41] performed model calculations using the SAMI2 code [64] to theoretically discuss the mechanism of occurrence features of the *F3* layer obtained through the statistical analysis and to examine the relationship between the *F3* layer and the equatorial anomaly. The SUPIM, SAMI2, and GSM TIP models take into account all processes that proposed to explain the equatorial *F2* layer stratification and the *F3* layer formation, namely, the electromagnetic plasma drifts, neutral wind, thermal plasma diffusion processes along geomagnetic field lines, thermal plasma sources, and losses.

**2.2. Latitudinal Dependence of the *F3* Layer.** Note that most studies of the *F3* layer are based on ionosonde observations of single or several stations located at three longitudinal sectors (American, Indian, and Pacific). Ionosondes are mainly separated by great distances in latitude. Therefore, the scanty spatial resolution of ground data is unable to give the refined spatial distribution of the *F3* layer. However, Lynn et al. [65] first presented the latitudinal dependence of the *F3* layer occurrence at the equatorial latitudes in South East Asia using the observations from a number of oblique and vertical ionosondes. They found that the region of maximum *F2* layer stratification lay between the magnetic equator and the peak of the southern EIA. Lynn et al. [65] also discussed the problem of the nomenclature to describe *F2*

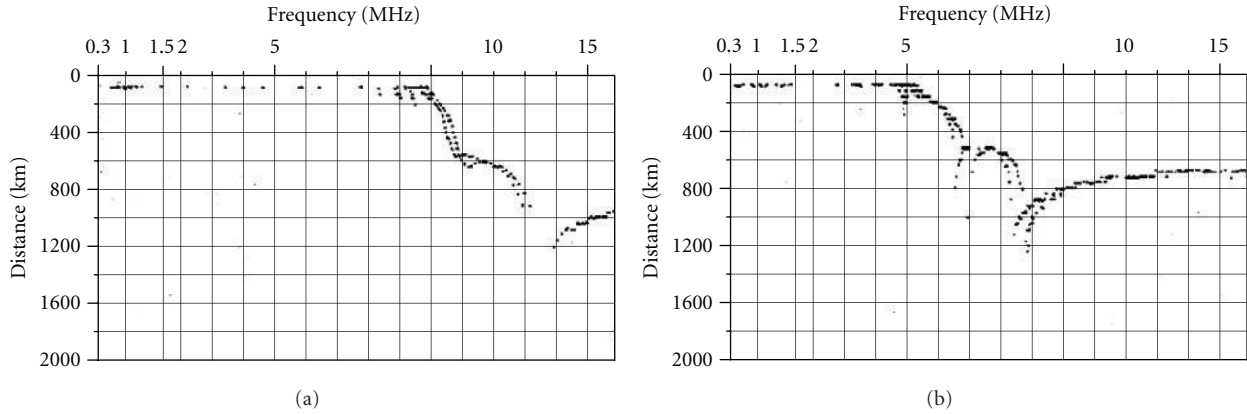


FIGURE 11: IK-19 satellite topside ionogram (from Karpachev et al. [52]) recorded: (a) at 23:16 UT (15:40 LT) on 25 November 1980 at the MLat  $-4.9^\circ$  and longitude  $245^\circ$  E, (b) at 16:04 UT (07:00 LT) on 7 September 1980 at MLat  $0.8^\circ$  and longitude  $223.3^\circ$  E.

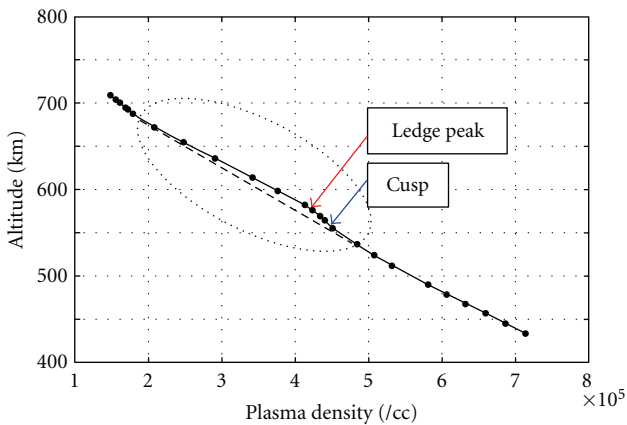


FIGURE 12: The  $N(h)$  profile reduced from the ionogram obtained on-board the Ohzora (EXOS-C) satellite at  $284.2^\circ$  E long.,  $0.5^\circ$  N dip lat. At 12.0 LT in March 17, 1987 (from Uemoto et al. [49]). Vertical and horizontal axis indicate the altitude and the plasma density, respectively. The red arrow gives the peak of the ledge structure. The blue arrow indicates and the height corresponding to the cusp.

layer stratification. The stratification was described in terms of a kink in the  $F2$  profile, which could rise above the peak of the background  $F2$  layer or remain below the peak depending on the latitude of observation. They proposed that the additional layer be referred to as an  $F3$  or an  $F1.5$  depending on whether the transitory layer moved above or stayed below the  $F2$  layer peak which maintained continuity with the pre- and poststratification  $F2$  layer. This latitudinal effect was suggested as arising from the kink in the profile mapping down the field lines with increasing distance from the magnetic equator. Their oblique ionosonde measurements in Southeast Asia show that the transitory layer was seen as an  $F3$  layer close to the magnetic equator but invariably as an  $F1.5$  layer farther from the magnetic equator. These observations suggest that the distortion in the equatorial electron density profile associated with a movement toward

the base of the  $F2$  layer as magnetic field lines descended with increasing latitude.

A comparative study by Rama Rao et al. [39] has also been carried out with ionograms recorded at an equatorial station Trivandrum ( $8.5^\circ$  N,  $76.9^\circ$  E;  $0.5^\circ$ ), India, and another low latitude stations Sriharikota (SHAR) ( $13.8^\circ$  N,  $80.3^\circ$  E;  $6.8^\circ$ ), India, and at Waltair ( $17.7^\circ$  N,  $83.3^\circ$  E;  $8.2^\circ$ ), India. They have shown that, on many occasions,  $F3$  layer was observed at Waltair without additional stratification in the  $F2$  layer either at SHAR or at Trivandrum. Thus it is observed that the occurrence of the  $F3$  layer is stronger at Waltair, weak at SHAR, and minimum or almost absent at Trivandrum, indicating that the latitude of Waltair could be the most favorable location over India for the formation of the  $F3$  layer.

Another indirect method to estimate the latitude dependence of the  $F3$  layer occurrence was through an investigation of long-term ionogram data at an equatorial station Fortaleza ( $4.0^\circ$  S,  $38.0^\circ$  W), Brazil [38], which shows that the  $F3$  layer occurrence decreases with decreasing dip angle. The maximum occurrence appears during 1995–1998 while magnetic dip angle lies in  $-8.9^\circ \sim -10.4^\circ$ . Also, the position of the appearance of the  $F3$  layer is investigated through the single station  $TEC$  measurements using radio beacon transmissions from low earth orbiting (LEO) satellites [54]. They have found a hump structure in the latitude variation of vertical  $TEC$  centered at magnetic latitude  $7 \sim 8^\circ$  at longitude  $\sim 80^\circ$  E. Zhao et al. [55] present a statistical work to infer the  $F3$  layer structure directly from COSMIC/FORMOSAT-3 RO data. Statistical results show an accurate magnetic latitude dependence of the occurrence of the additional layer and reveal that the highest occurrence of  $F3$  layer appears at dip latitude  $\pm 8^\circ$  during summer months. Similarly, according to the ground-based data  $F3$  layer is observed rarely at the equator than at low latitudes  $\pm(7 \sim 8^\circ)$  [37, 39, 41, 65].

Recent studies show that the  $F3$  layer near the magnetic equator behaves in a different way than that in the magnetic low-latitude region [41, 43, 66]. The  $F3$  layer moves rapidly upward near the magnetic equator, while it stays almost at a certain altitude in the magnetic low-latitude region. The

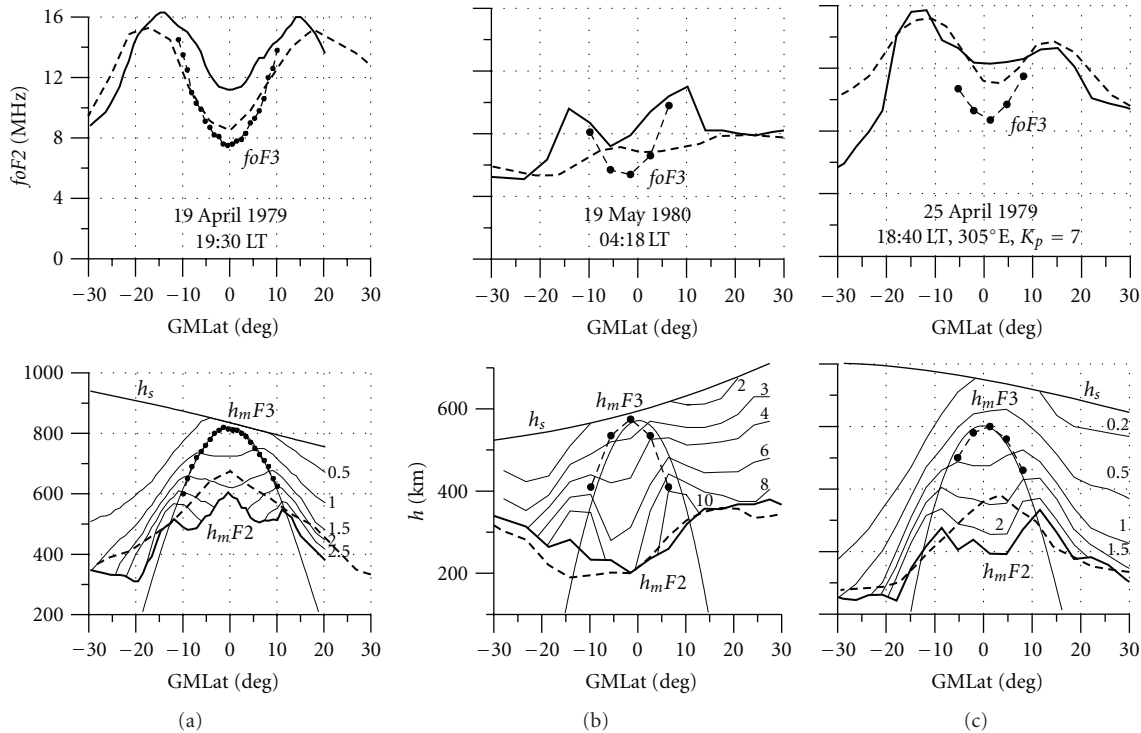


FIGURE 13: Latitudinal distribution of  $foF2$  (top) for quite time on 19 April 1979 (a), 19 May 1980 (b), and 25 April 1979 (c). Solid lines: at the ledge occurrence, thick dashed lines: without ledge on adjacent satellite passes, thin dashed lines with points:  $foF3$ . The bottom panel shows the same for  $hmF2$  and  $hmF3$ . Thick lines: geomagnetic field lines, thin lines: electron density contours ( $N_e$  in  $10^6 \text{ cm}^{-3}$ ),  $h_s$ : satellite height. The data and local time are indicated at all plots. From Karpachev et al. [52].

occurrence probability near the magnetic equator is less than 30%, that is, much lower than that in the low-latitude regions ( $\sim 70\text{--}80\%$ ). The occurrence is confined to the morning local time period near the magnetic equator and started to form at an earlier local time and lasts for a shorter period (1–3 hours) than in the magnetic low-latitude region.

On the topside sounding ionograms the ledge merges with the  $F2$  layer peak at magnetic latitudes of  $\pm 15^\circ$ . The ledge frequency decreases, and its height increases up to an altitude of  $\sim 1000$  km at the approach to the geomagnetic equator (see Figure 13) [18, 50, 52]. King et al. [19] and Lockwood and Nelms [18] showed the ionization ledge lying along the magnetic field line passing through the EIA crests. The same results were obtained by Raghavarao and Sivaraman [20] Uemoto et al. [50] with use of ISIS-2 satellite data, Uemoto et al. [49] with use of EXOS-C satellite data, and Karpachev et al. [52] with use of IK-19 satellite data (see Figure 13). However, Sharma and Raghavarao [22] suggested that until about 16:00 LT, both the peak of the ionization ledge and the anomaly crests are located aligned along the same field line, and then they become to be separated from each other. Uemoto et al. [50] also observed some of ledge structures showed that the peak of the ledge was connected to the magnetic field line of higher latitude side than the field line of the crest of the equatorial anomaly. So the ionization ledge occurs in a dip latitude range from  $-13.5^\circ$  to  $19.3^\circ$  according to Uemoto et al. [50] and from  $-10^\circ$  to  $10^\circ$  according to Karpachev et al. [52].

### 2.3. F3 Layer at Low Latitude Near the Magnetic Equator

**2.3.1. Diurnal Variations of the F3 Layer.** According to statistical studies by Balan et al. [35], Rama Rao et al. [39], and Sreeja et al. [43] based on a day-to-day ionosonde data, the  $F3$  layer occurs as early as 08:00 LT to as late as 17:00 LT and lasts for as little as 15 min to as long as 6 hours. Zhao et al. [66] investigated characteristics of the sunset  $F3$  layer using a solar cycle of ionosonde data (1995–2010) from the magnetic equatorial station at Jicamarca (see Figure 15) and compared with the features derived from the four subtropical stations at Sao Luis ( $2.6^\circ\text{S}$ ,  $44.2^\circ\text{W}$ ;  $-2.0^\circ$ ), Brazil, Fortaleza ( $4.0^\circ\text{S}$ ,  $38.0^\circ\text{W}$ ;  $-6.6^\circ$ ), Brazil, Kwajalein ( $9.0^\circ\text{N}$ ,  $167.2^\circ\text{E}$ ;  $3.8^\circ$ ), Marshall Islands and Vanimo ( $2.7^\circ\text{S}$ ,  $141.3^\circ\text{E}$ ;  $-11.2^\circ$ ), Papua New Guinea. Evidence shows that the local time distribution of the occurrence of the  $F3$  layer can extend to the postsunset time (18:00–21:00 LT). Unlike the daytime  $F3$  layer, the occurrence of the sunset  $F3$  layer clearly increases with increasing solar activity.

The studies of the diurnal variations in ionization ledge occurrence probability with use of satellite data are scarce, since they require a sufficiently large database. Figure 16 shows the local time dependence of the ionization ledge occurrence probability [50], derived from the analysis of 430 passages of ISIS-2 satellite in 1973–1977. It is evident that during low solar activity the ionization ledge is observable almost all local time sectors except for the period from 03:00 to 08:00 LT sector. The occurrence probability of the

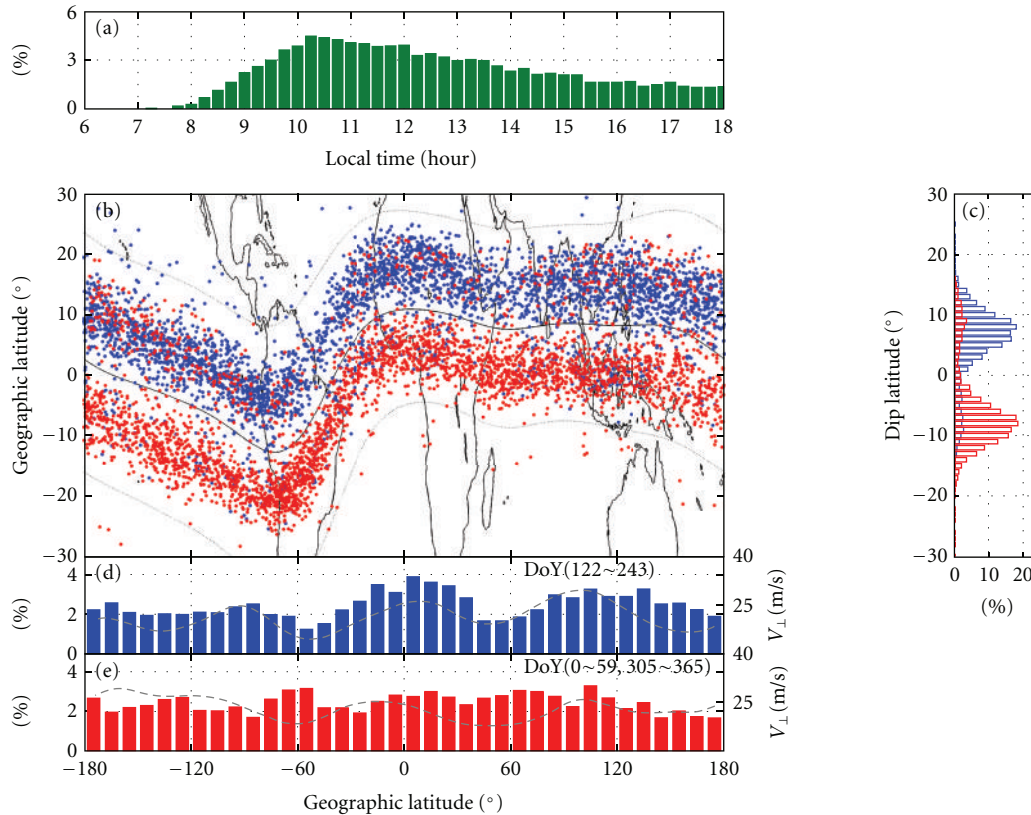


FIGURE 14: *F3* layer occurrence as a function of (a) local time, (b) geographic position of the *F3* layer during 06:00–18:00 LT in boreal summer (blue) and winter (red), (c) dip latitude, (d) geographic longitude during boreal summer, and (e) winter. ROCSAT-1-derived equatorial vertical drift  $V_{\perp}$  (gray) was superimposed on (d) and (e) (from Zhao et al. [55]).

ionization ledge is highest at noon local time sector and tends to decrease gradually as the time progresses. Raghavarao and Sivaramam [67] concluded that the topside ledges occurred more frequently and lasted longer into the night during sunspot minimum period than at sunspot maximum. The same conclusion was made regarding the appearance of *F3* layer according to ground-based sounding data [43].

Diurnal variations in the height of the ionization ledges were investigated according to the Alouette-1 satellite data [18]. The ledges were observed from 11:00 to 22:00 LT. The height of ledges increased with time from 450 to 900 km. The ledges were also observed after 22:00 LT, but spread *F* prevented their detection. Uemoto et al. [49, 50] found contradictory results on the diurnal variation in ionization ledge height (see Figure 17). According to the EXOS-C (Ohzora), the ionization ledge rapidly rises from  $\sim 500$  km at 11:20 LT to  $\sim 950$  km at 14:20 LT, but the ISIS-2 satellite data show a scattered nature in the ledge local time dependence.

Figure 18 shows the diurnal variations in *F3* layer height obtained from the IK-19 satellite data for all seasons just over the geomagnetic equator, which is compared with dashed line, indicating the ground-based sounding data in South-East Asia for high solar activity [65], and with the closed contour outlining the Alouette-1 satellite data for low solar activity [18]. The ground-based sounding data show that the *F3* layer appears at 07:00–08:00 LT and its height increases

rapidly to 12:00–13:00 LT [36, 39, 65] as evident from Figure 18. At this time the *F3* layer is better developed than the *F2* layer and thus recorded in sounding data. In this case the satellite records the *F3* layer as the *F2* layer. The IK-19 satellite as all other ones recorded the *F3* layer only if  $foF3$  did not exceed  $foF2$ . The *F3* layer formation and its height growth are closely associated with an increased velocity of vertical plasma drift that revealed by ROCSAT-1 satellite data [68] shown in Figure 18. At 12:00–13:00 LT the situation is reversed, ground-based stations no longer detect the *F3* layer, and topside sounders detect the *F3* layer on a regular basis. Alouette-1 satellite regularly recorded the *F3* layer only at 11:00–12:00 LT, but at much lower altitudes than those of the IK-19. This is due to the fact that the observations of these two satellites relate to different levels of solar activity. Both the IK-19 and Alouette-1 satellites recorded sharp increase in  $h_mF3$  up to 900–950 km at 20:00–21:00 LT. This is related to the EIA increase in this period that shows the curve for the equatorial anomaly intensity (EAI). This contradicts to the conclusions of King et al. [19] which show a maximum height of ledges ( $\sim 850$  km) at around 16:00 LT, but is fully consistent with the results of Uemoto et al. [49] based on the EXOS-C data. Lockwood and Nelms [18] did not detect the *F3* layer after 22:00 LT due to strong spread *F*. Actually, the strong spread *F* events were observed at nighttime equatorial ionograms of IK-19

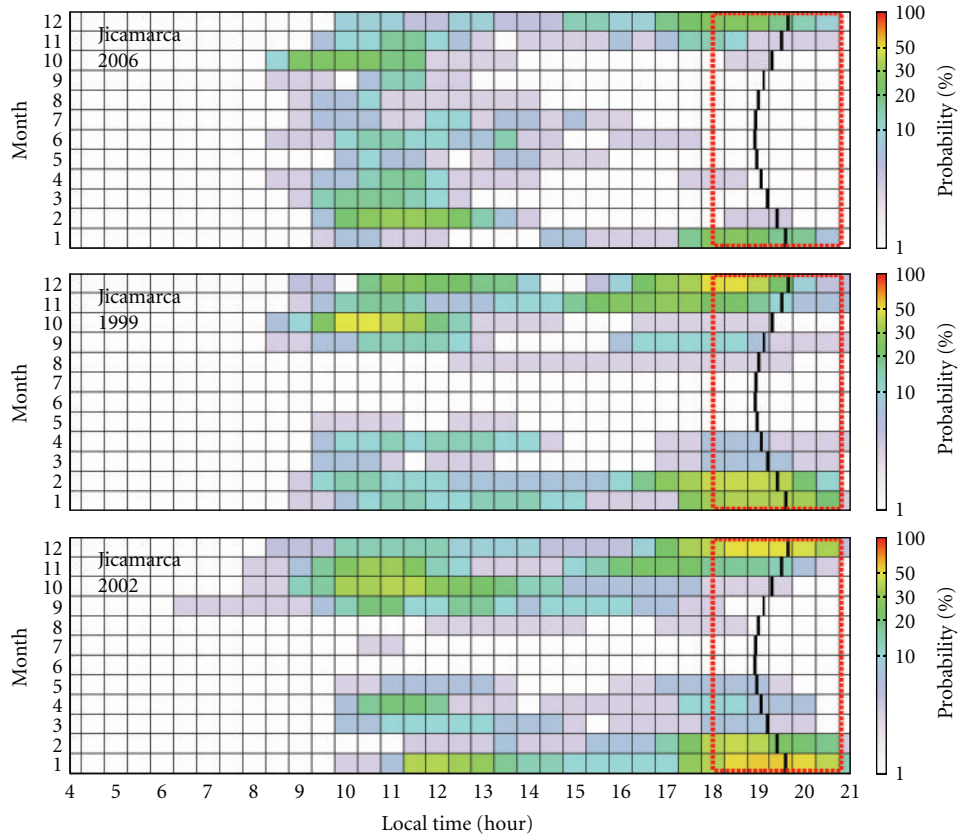


FIGURE 15: Occurrence probability of the  $F_2$  layer stratification at Jicamarca during low, medium, and high solar activity. The solar terminator around sunset (thick line) at 300 km is shown.

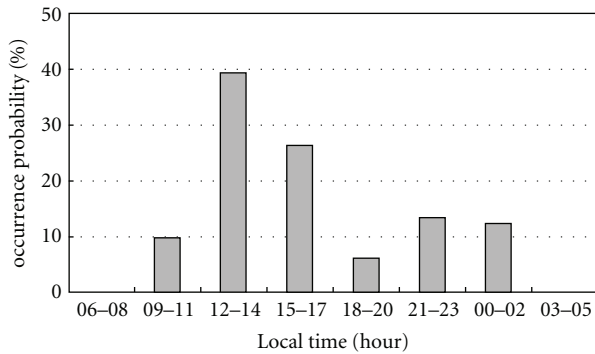


FIGURE 16: Local time dependence of the occurrence probability of the ionization ledge based on the ISIS-2 data analysis (from Uemoto et al. [50]).

satellite, so that approximately one third-part of nighttime ionograms cannot be processed. However, a large database of IK-19 allows recording the bright cases of the nighttime  $F_3$  layer occurrence. The nighttime  $F_3$  layer (04:00 LT) was first detected according to the IK-19 data by Depuev and Pulinets [51]. Figure 13(b) shows a well-developed  $F_3$  layer at night, when the EIA is poorly developed. From Figure 18 it is evident that the  $F_3$  layer height falls to the morning hours

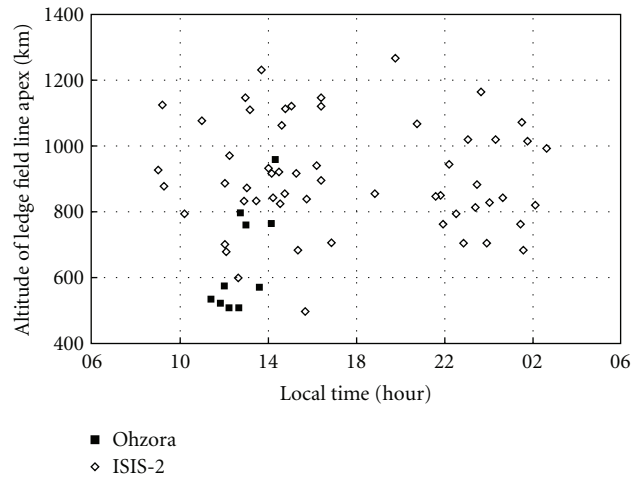


FIGURE 17: Squares and diamonds indicate the location of the ionization ledge observed from the Ohzora and the ISIS-2 satellites, respectively (from Uemoto et al. [50]).

(05:00–07:00 LT) to ~450 km. The curve for EAI shows that EIA at this time is usually absent.

2.3.2. *Longitude Dependences of the  $F_3$  Layer Occurrence.* Raghavarao et al. [21] revealed that the ledges are seen to

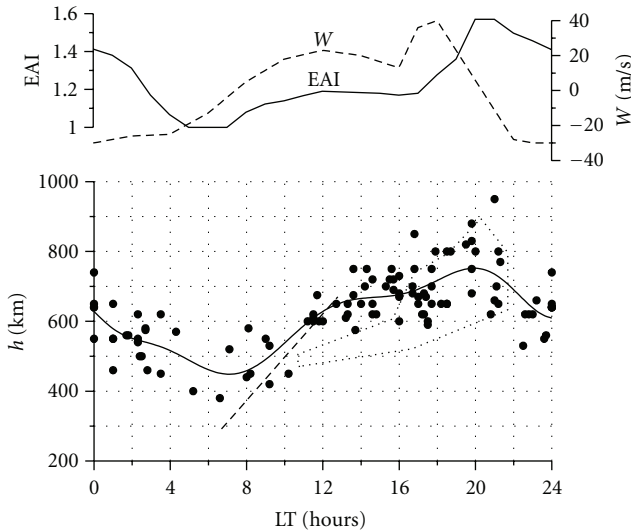


FIGURE 18: Bottom panel:  $h_m F3$  diurnal variation. The points show the IK-19 data, the solid line: approximation of the IK-19 data, the dashed line: virtual height of the  $F3$  layer from ground-based ionosonde data [65]. Closed contour outlines a data array of Alouette-1 with ionization ledge occurrence according to Lockwood and Nelms [18]. Top panel: variation in vertical plasma drift velocity  $W$  over the equator [68] and the equatorial anomaly intensity (EAI).

occur with different intensity at two close-by longitudes. The longitudinal variations of the ledge occurrence probability can be studied only on the basis of IK-19 satellite data that have not already done. The longitudinal variations of the  $F2$  layer parameters above the equator with use of IK-19 satellite data were obtained in [69–71]. Deminova [71] has devoted 3 or 4 harmonics in  $foF2$  and  $h_m F2$  in the EIA region regardless of local time (in the interval 17:00–05:00 LT). Variations in  $N_e$  in the external equatorial ionosphere, with wave numbers (WN) 3 and 4 were also described in [72]. The concept of four harmonics “WN4” in recent years is widespread. According to this concept four harmonics in the longitudinal variations of the equatorial ionospheric parameters are created by nonmigrating tidal waves coming from the lower atmosphere. They modulate the electric field at the  $E$  region heights, which is transmitted to the  $F2$  layer heights and causes the  $\mathbf{E} \times \mathbf{B}$  plasma drift (see the recent paper [73] and references therein).

Zhao et al. [55] have inferred from the COSMIC data that the  $F3$  layer occurrence has a longitude dependence during boreal summer, with relatively higher occurrence at  $-80^\circ \sim -100^\circ$ ,  $-20^\circ \sim 20^\circ$ ,  $80^\circ \sim 120^\circ$ , and  $-160^\circ \sim -170^\circ$  longitudes (see Figure 14), which is possibly associated with the wavenumber-3 diurnal tide (DE3). In fact, the linkage between the stratification of  $F2$  layer and tides in the low thermosphere has been investigated 50 years ago. Osborne [6] reported that the phenomenon of the “spur” at Singapore was related to lunar time and represented an upward-moving layer based on the measurement in 1948–1951. M. V. Klimenko and V. V. Klimenko [47] showed that, to reproduce  $F3$  layer phenomenon in global self-consistent

thermosphere-ionosphere model calculations, it is necessary to account the thermospheric tides. So more ground and satellite observations and model studies needed to clarify the longitude dependences of the  $F3$  layer occurrence.

**2.3.3. Inconsistency of the Observation on the Seasonal Dependence of the  $F3$  Layer.** It was reported that in Fortaleza, Brazil ( $4.0^\circ\text{S}$ ,  $38.0^\circ\text{W}$ ;  $-4.4^\circ$ ), the  $F3$  layer in 1995 occurs frequently not only in the local summer but also in winter seasons and is less frequent in the equinox seasons [35, 38]. According to the observation at Ibadan ( $7.4^\circ\text{N}$ ,  $3.9^\circ\text{E}$ ;  $-2.1^\circ$ ), Nigeria during 1951–1953, Skinner [7] found that there are more morning  $F3$  layers in winter than in summer. Zhao et al. [66] have also presented the statistical result at Fortaleza using the data during 2007–2010 which shows much lower occurrence in winter different from the result of Balan et al. [35] based on the data during 1995. It should be noted that the magnetic latitude of Fortaleza changes from  $-4.4^\circ$  to the present  $-7.0^\circ$  and the calculation of the occurrence probability is different. According to Balan et al. [35], the  $F3$  layer winter occurrence though high lasts for very short period during the morning local time when  $\mathbf{E} \times \mathbf{B}$  drift is very effective. The sunset  $F3$  layer has a strong seasonal dependence occurring mainly during the summer time [66]. The contradiction in the statistical result may also partly suffer from the fact that the judgment of the stratification of  $F2$  layer is very subjective and no uniform standard has been applied to judge the difference between the fully developed and unfinished stratification. Further study involved with the station Fortaleza is needed to reveal its peculiarity.

On the other hand, Rama Rao et al. [39] examined the variation of the occurrence probability of the  $F3$  layer in Waltair, India ( $17.7^\circ\text{N}$ ,  $83.3^\circ\text{E}$ ;  $8.2^\circ$ ), and showed that the  $F3$  layer frequently occurs in the local summer season as well as equinox seasons and is less frequent in the local winter season. The statistic of the  $F3$  layer occurrence at Chiang Mai ( $18.8^\circ\text{N}$ ,  $98.9^\circ\text{E}$ ;  $13.2^\circ$ ), Thailand resembles that of Indian result [41]. The statistic of the  $F3$  layer occurrence at Chumphon ( $10.7^\circ\text{N}$ ,  $99.4^\circ\text{E}$ ;  $3.2^\circ$ ), Thailand resembles that of at Kwajalein ( $9.0^\circ\text{N}$ ,  $167.2^\circ\text{E}$ ;  $3.8^\circ$ ) of Zhao et al. [66]. Thus these results suggest that the difference in seasonal dependence of the occurrence probability between Indian and Brazil may not be mainly caused by the difference of the geographic longitude but that of the magnetic latitude. In addition the hemispheric asymmetry of the seasonal  $F3$  layer occurrence should also be considered. Uemoto et al. [41] showed that at Kototabang ( $0.2^\circ\text{S}$ ,  $100.3^\circ\text{E}$ ;  $-10.1^\circ$ ), Indonesia the summer occurrence probability was higher than that at Chiang Mai. They suggest that the summer-to-winter wind is strong in the southern hemisphere than in the northern hemisphere because the magnetic equator is shifted northward from the geographic equator in Southeast Asia by approximately  $10^\circ$ . Thus further study needs to be carried out to elucidate the hemispheric asymmetry at the other longitudes that has large discrepancy between the geomagnetic and geographic equator.

The seasonal variations of ionization ledge occurrence probability according to the topside sounding data from

ISIS-2 satellite were shown only in a single study [50]. According to the ISIS-2 satellite data, the ledge is most often observed at the equinox and in autumn more often than in spring, less in summer, and much less in winter. Uemoto et al. [50] have concluded that, although the characteristics of the ionization ledge and the  $F3$  layer are similar, their seasonal dependence is, in general, different.

**2.3.4. Mechanism of the Quiet-Time  $F3$  Layer.** Balan and Bailey [32, 35] proposed that the combined effect of the upward  $\mathbf{E} \times \mathbf{B}$  drift and neutral wind provides vertically upward plasma velocity at altitudes near and above the  $F2$  peak. The vertical velocity causes the  $F2$  peak to drift upward and form the  $F3$  layer while the normal  $F2$  layer develops at lower altitudes through the usual photochemical and dynamical processes of the equatorial region. It looks very close to the mechanism of Huang [15] which proposed that the formation of  $F2$  layer stratification is principally due to the combined effect of the upward drift, which changes from increasing to decreasing at 10:00 LT, and the slow diffusion. This mechanism can well explain most  $F3$  layer features observed at low and equatorial areas. Jenkins et al. [34] showed that the observed stratification of the  $F2$  layer cannot be the signature of a propagating disturbance such as that caused by a gravity waves. Jenkins et al. [34] demonstrated the role of transequatorial winds as a necessary condition for the formation of the  $F3$  layer in summer and winter conditions in the minimum of solar activity. Although the neutral wind controls where and when the  $F3$  layer appears with higher probability, the main driving force for the formation and maintenance of the  $F3$  layer is the upward  $\mathbf{E} \times \mathbf{B}$  drift velocity (see Figure 19) [34, 35].

The mechanism of the  $F3$  layer formation, suggested in [35], looks as follows. Early in the morning there is a usual  $F2$  layer. With the progress of time it becomes wider due to the effect of photoionization and unique dynamic effects in the equatorial region. Due to the dominance of  $\mathbf{E} \times \mathbf{B}$  drift at the geomagnetic equator, the peak of the layer at the equator moves up faster than at other latitudes. While being transported upward, this maximum passes through the region in which chemical and dynamic processes are equally important and gets into the region where dynamic processes dominate. After some time and below this peak, a new maximum is formed in the region of balance of chemical and dynamic processes. The top maximum becomes a maximum of the  $F3$  layer which after some time disappears due to chemical losses and diffusion, which dominate over ionization processes at these heights. It is possible to discuss the reasons for the disappearance of  $F3$  layer due to chemical losses and diffusion. There is no doubt the role of diffusion in the decrease of plasma density at the peak of  $F3$  layer during its lifting to the larger heights. This is due to diffusion redistribution of the plasma from the top of the plasma tube down along the geomagnetic field lines. Involvement of chemical losses to explain the fall of the plasma density at the peak of  $F3$  layer at its upward movement toward the region with lower rates of loss seems unjustified. Note that the rate of chemical losses (in the  $F$ -region ionosphere) decreases

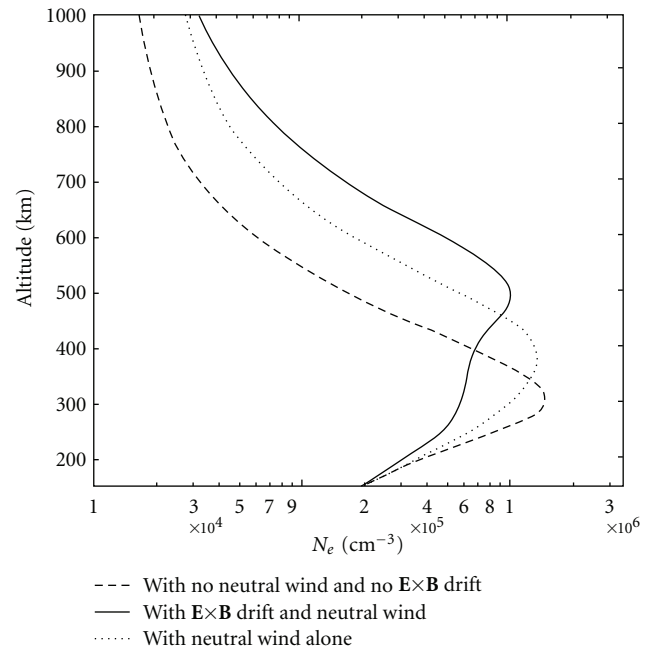


FIGURE 19: Electron density profiles from model calculations with  $\mathbf{E} \times \mathbf{B}$  drift and no neutral wind (dashed curve), with neutral wind and no  $\mathbf{E} \times \mathbf{B}$  drift (dotted curve), and with both  $\mathbf{E} \times \mathbf{B}$  drift and neutral wind (split curve) (from Balan et al. [35]). The profiles correspond to 11:00 LT at  $4^\circ$  magnetic latitude at the longitude of Fortaleza during June solstice at low solar activity. Note that the  $F3$  layer does not form when the wind alone is used (dotted curve).

with height much faster than the rate of ion production. Thus, the drop in plasma density at the peak of  $F3$  layer when it moves upward under the influence of the eastward electric field occurs only due to diffusion.

Uemoto et al. [41] improve the mechanism of Balan et al. [35] by claiming that the field-aligned diffusion of plasma acts to make the  $F3$  layer prominent in the magnetic latitude far off the magnetic equator region (more than  $7^\circ$ ). Also Uemoto et al. [40, 41] show ionosonde observations of the  $F3$  layer in both the winter and summer hemispheres concurrently. This is explained by plasma diffusion from the magnetic equator to the low-latitude regions due to the pressure gradient and the gravitational force. Early Raghavarao and Sivaraman [67] suggested and Surotkin et al. [31] demonstrated that the physical cause of the formation of  $F2$  layer stratifications is nonuniform diffusive plasma outflow from the region over the magnetic equator at the equatorial anomaly crests developed.

However, Thampi et al. [54] proposed that an upward  $\mathbf{E} \times \mathbf{B}$  drift and strong equatorward neutral wind (perturbed by AGW) can produce the humps in the latitudinal variation of  $TEC$  through the reduction in the downward diffusion of ionization along geomagnetic field lines. The hump is associated with  $F3$  layer observed in the ground ionosonde. Their model result shows that an upward  $\mathbf{E} \times \mathbf{B}$  drift with ordinary neutral wind cannot produce the humps in the latitudinal variation of  $TEC$  as in the observation. The

mechanism suggested by Thampi et al. [54] resembles that of Fagundes et al. [26] for the EIA region. However, they have not calculated the wave parameters through the ionosonde data to rule out possibility of the ordinary  $F3$  layer which have the following signature: (a) it remains at the same virtual height and does not propagate downward to lower frequencies as a gravity wave would be expected to do; (b) no periodicity is observed in the intensity of the cusp.

Balan et al. [35] concluded that the  $F3$  layer is formed in the morning and daytime sector, when the ionization processes dominate over chemical losses due to upward plasma transport under the action of  $\mathbf{E} \times \mathbf{B}$  drift and neutral wind. There is a question. Can the  $F3$  layer occur at nighttime and during sunset? If yes what is the mechanism of it? The strength and direction of the equatorial zonal electric field undergoes large day-to-day variability [36]. Fejer et al. [74] gave the average pattern of the equatorial  $F$  region drift, which shows that the upward  $\mathbf{E} \times \mathbf{B}$  drift increases from morning hours to noon, during which the  $F3$  layer can be best seen. Another period during which the  $F$  region undergoes a quick ascent is around dusk when the prereversal enhancement (PRE) of the eastward electric field develops. Balan et al. [35] suggested that although the driving force undergoes a large and sudden upward strengthening during the evening hours, formation of another layer at lower altitudes is unlikely to occur when the  $F2$  layer drifts upward, because of the absence of the production of ionization. However, Depuev and Pulnits [51], Karpachev et al. [52], and Zhao et al. [66] described the case of the  $F3$  layer occurrence at night (00:00–04:00 LT) and at post sunset time (18:00–21:00 LT at Figure 15). Klimenko et al. [46] and M. V. Klimenko and V. V. Klimenko [48] demonstrated that the  $F3$  layer is formed as a result of the nonuniformity in height vertical  $\mathbf{E} \times \mathbf{B}$  plasma drifts at the geomagnetic equator. The height gradients in vertical plasma drifts were previously observed by incoherent scatter radar over Jicamarca [75]. This mechanism can explain the  $F3$  layer occurrence at different LT epochs (especially at night). The occurrence of the sunset  $F3$  layer at Sao Luis (2.6°S, 44.2°W;  $-2.1^\circ$ ) is much less than that at Jicamarca ( $-0,6^\circ$ ) although the PRE drift for the former is more significant than that of the latter [66]. The combined effects of the PRE electric field and the equatorward wind and geomagnetic configuration allow the  $F3$  layer to be observed more frequently at Jicamarca than at the Sao Luis longitude, which has a large magnetic declination of  $-18^\circ$ . Thus the mechanism of the  $F2$  layer stratification is still an open question in the low latitude and we do not know which is dominant that well explained the observed phenomenon.

**2.3.5. Storm-Time  $F3$  Layer Feature.** Numerous studies have demonstrated that the geomagnetic storm affects the formation of additional layer in the low-latitude  $F$  region. Zhao et al. [76] found that the noon time stratification of the  $F2$  layer at magnetic equator became severe during the Halloween storm in 2003 that is related to the prompt penetration electric field (PPEF) originated from the magnetospheric convection electric field. Paznukhov et al. [77] presented

such a case at Jicamarca during the superstorm November 9–10, 2004. Sreeja et al. [57] showed the development of  $F3$  layer at dawn and dusk local time due to the PPEF. Balan et al. [78] considered the data from three longitudes (Japan-Australian, Indian, and Brazilian regions) and for 22 storms in 11 years (1998–2008) and showed that the existence of  $F2$  stratification during the main phase of the storm is a standard feature of the equatorial ionosphere and serve as an indicator of the storm-time PPEF.

The mechanism responsible for the storm time  $F3$  layer is similar to that in quiet periods but with a much faster processing time due to the rapid uplift of the  $F$  layer by an upward  $\mathbf{E} \times \mathbf{B}$  drift resulting from an eastward penetration electric field. Balan et al. [56] and Lin et al. [59] presented a theoretical model of this process in detail based on the thermosphere ionosphere electrodynamics general circulation model (TIEGCM) and SUPIM. These studies indicate that the additional layer becomes more prominent and more distinct during geomagnetic disturbances than in quiet conditions. Balan et al. [56] reported an interesting storm feature of the equatorial ionosphere profile associated with a strong eastward PPEF followed by a westward electric field. By incorporating the fluctuated measured  $\mathbf{E} \times \mathbf{B}$  drift in the SUPIM, they have shown the development of unusually strong  $F3$  layer that quickly ascends to the topside ionosphere during the afternoon period of PPEF. The  $F3$  layer then drifts downward due to a westward electric field that merged with  $F2$  layer.

Through the GSM TIP model, Klimenko et al. [45, 46] proposed that an alternative formation mechanism of the  $F3$  layer is nonuniform in height distribution of zonal component of an electric field (see Figure 20). It causes the nonuniform vertical plasma drift that leads to plasma convergence at some altitudes and to its rarefaction at others. The formation mechanism will even produce  $F4$  layer during the storm time but at larger heights according to the modeling results. The formation mechanism of the  $F4$ -layer is the same as the  $F3$  layer. They showed that geomagnetic storms affect the formation, existence, lifetime, and the number of additional layers in the equatorial ionosphere.

Lockwood and Nelms [18] investigated the dependence of the ledge occurrence from the magnetic activity and found that the  $F3$  layer occurs later during storm-time than in quiet days. Karpachev et al. [52] considered the  $F3$  layer occurrence during 10 magnetic storm events under  $K_p = 5-8$  with use of IK-19 satellite data. Observations for all storms were sufficiently prolonged (10 passes or about 17 hours). This allows recording the  $F3$  layer appearance during the storms both in the daytime and nighttime sectors. These data analyses showed that the  $F3$  layer was absent in two cases, poorly seen in five cases, and appeared sufficient clearly only in three cases. Figure 13(c) shows the IK-19 example of  $F3$  layer occurrence during a strong geomagnetic storm ( $K_p = 7$ ) on April 25, 1979. Note that in quiet periods we can observe more pronounced examples of the additional layer. Thus, the  $F3$  layer is not always formed even during strong magnetic storms. However, according to ground-based sounding data, the  $F3$  layer appears more often in the disturbed days [43].

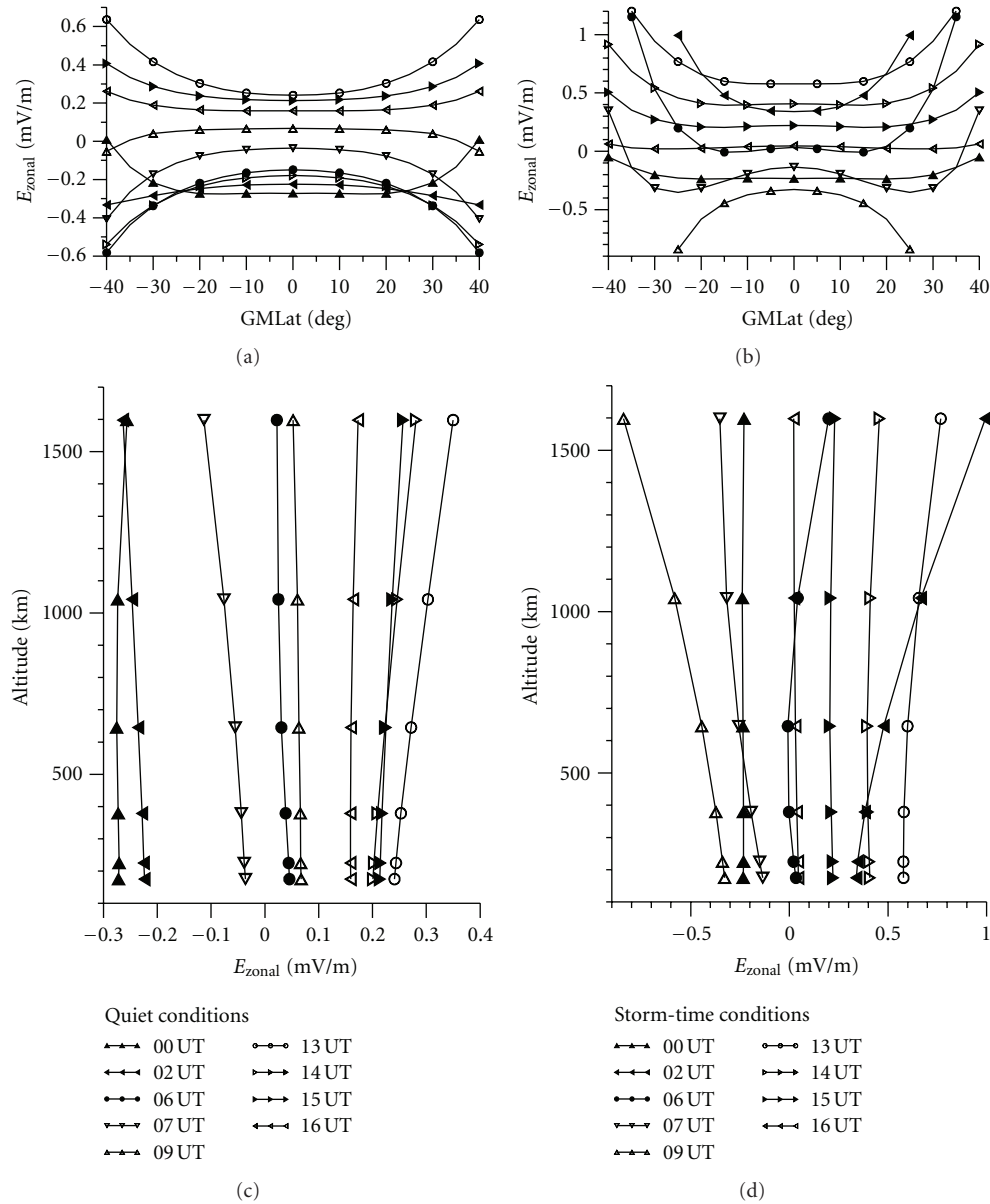


FIGURE 20: Latitudinal profiles of zonal electric field in the geomagnetic longitude of station Jicamarca (top) and vertical profiles of zonal electric field above station Jicamarca at the different UT epochs obtained in model calculations for quiet and storm time conditions. (from Klimenko et al. [45]).

2.4. *F3 Layer Features over the EIA Region.* Fagundes et al. [26] reported daytime *F2* layer stratification over an equatorial anomaly crest location at Sao Jose dos Campos (23.2°S, 45.9°W; -17.6°), Brazil. This type of *F2* layer stratification seems to be associated with a possible manifestation of middle scale travelling ionospheric disturbances (MSTIDs) due to the propagation of atmospheric gravity waves (AGWs) in the middle latitudes [8]. They have made a statistical study based on the ionogram data from September 2000 to August 2001 which shows that the *F3* layer occurs only for 66 days (18% occurrence), and it occurs only during September–February (spring-summer), with maximum occurrence in September–October and longest duration in February. The

calculated periods of AGWs are about 30–60 min, downward phase velocities of about 60–140 m/s, and vertical wavelengths of about 200–500 km. The duration of this type of stratification is 1–2 hours which is much longer than that usually observed in the middle latitudes.

Fagundes et al. [79] investigate the occurrence of *F3* layer formation as a function of solar cycle and season near the EIA southern crest in Brazil. They have shown that (I) the frequency of occurrence during high solar activity (HSA) is 11 times greater than during low solar activity (LSA), (II) during HSA there is a maximum occurrence of *F3* layer during summer time and a minimum during winter time; while during LSA there is no seasonal variation in the *F3*

layer occurrence, and (III) during the maximum occurrence season in HSA  $F3$  layer was generated almost every day and lasted for several hours, while during the month with minimum occurrence, the  $F3$  layer lasted for about one hour or even less time. The seasonal and solar activity dependence of the  $F3$  layer occurrence suggests that the vertical extension of the  $F2$  layer is an important factor that is favorable for the formation of the  $F3$  layer if AGWs mechanism works, that is the  $F$  layer vertical extension must be larger than the gravity wave wavelength to create favorable conditions for stratification and formation of the  $F3$  layer [26]. During the HSA and summer season, large daytime upward  $\mathbf{E} \times \mathbf{B}$  drift and/or large equatorward wind can cause unusual vertical extension of the  $F2$  layer near the EIA crest. The upward propagating gravity waves in such an unusually extended  $F2$  layer seem to be the possible reason for the  $F2$  layer stratification and  $F3$  layer observed near the EIA crest.

It should be noted that study of Fagundes et al. [26, 79] is quite different from those reported by Abdu et al. [80] at the same site. Their study shows the effects of gravity waves in the  $F$  layer during the daytime and geomagnetic quiet conditions, whereas Abdu et al. [80] studied its effects during the nighttime with passage of TIDs possibly associated with geomagnetic disturbances. By using the TIEGCM and SUPIM runs during the major magnetic storm of 29–30 October 2003, Lin et al. [59] present a new type of additional layer in the evening which occurs in the EIA region by a new physical mechanism. This mechanism requires that storm time meridional neutral wind surges travel from high to low latitudes and cross into the opposite hemisphere. The wind surges modify the field-aligned plasma velocities in the EIA regions significantly after uplift of the ionospheric layer by a PPEF and interact with the downward field-aligned plasma velocities of the enhanced equatorial fountain. The combined storm effects of the enhanced plasma fountain and the neutral wind surges result in plasma convergence in altitude and form the additional layers underneath the EIA crests. Although such surge is reproduced by Klimenko et al. [45] during geomagnetic storm on September 11, 2005, it does not lead to the formation of additional layer above EIA crest. It is necessary to note that thermospheric wind surge was formed in Lin et al. [58] at night, but in Klimenko et al. [45] in the afternoon. Therefore, our modeling effort suggests that the additional layer in the area of equatorial anomaly crests is not formed by thermospheric wind surge in the daytime sector.

Another unclear issue is the longitude difference of the  $F3$  layer occurrence that lies in the EIA region. Occurrence of the  $F3$  layer is rare over Ahmedabad (23.0°N, 72.6°E, 14.4°), India and Chung-Li (25.0°N, 121.2°E; 19.7°N), Taiwan located under the northern crest of the EIA in Indian and East-Asian longitudes [37, 39], while is much higher at Sao Jose dos Campos (23.2°S, 45.9°W; -17.6°), Brazil. It is not known that this diversity is due to the AGW source regional difference like the tropospheric wind disturbances or simply to the ionospheric vertical structure difference. Except for the direct propagation of AGWs, the other processes which couple upward propagating tides, planetary waves with ionospheric changes also affect the  $F3$  layer probability, for

instance, through modification of turbulent mixing and hence  $O/N_2$  ratios, influences on  $E$  region conductivities, modulation of the temperature and wind structure of the thermosphere, and the generation of electric fields through the dynamo mechanism [81].

### 3. Puzzles that Need to be Clarified in the Future Studies

The characteristics of the  $F2$  layer stratification and its dynamics, topside ionization ledge and  $F3$  layer have been greatly clarified by old and recent observation and model studies, but there are still several remaining questions.

(1) One such big question regards the seasonal, solar activity, latitudinal, and longitudinal dependence of the  $F3$  layer. Now it is very difficult to separate these dependencies, since they are closely related. In order to clarify the spatial structure and seasonal dependence of the  $F3$  layer the statistical analysis ground-based sounding data, such as [26, 39–41, 43, 79], topside sounders (the large IK-19 data base is of special interest due to the presence of long periods of continuous observation), radio beacon measurements from low Earth orbiting satellites as [54], and RO technique as [55] are needed in the future studies.

(2) The second problem needing to be clarified in the future is the relationship between the topside ledge and ground-based  $F3$  layer. Uemoto et al. [50] claimed that the topside ledge may be regarded as a remnant of the ground-based  $F3$  layer due to the same mechanism of large  $\mathbf{E} \times \mathbf{B}$  drift. However, the seasonal dependence of the occurrence probability of the ionization ledge shows contradict manner to the  $F3$  layer. Neither the ground ionosonde nor the topside sounding technique can give a full picture of the evolution of the  $F2$  layer stratification (e.g., see Figure 21). Ground-based sounding data record the  $F3$  layer only when the electron density at its maximum is larger than the maximum of the  $F2$  layer. The satellite records only one-layered pattern (the  $F3$  layer) in this case. The researchers that used topside sounding satellite data mistakenly assume that it is the  $F2$  layer due to the lack of visible  $F2$  layer stratifications. It is important to understand that the  $F3$  layer may also exist in the absence of stratifications on ionograms. If the stratifications are absent on the topside sounding ionograms, we observe one layer, and it can be either the  $F2$  layer, or  $F3$  layer. If the stratifications are absent on the ionograms of ground-based sounding, it does not necessarily mean that the additional layers are absent. This could also mean that the electron density at the  $F2$  layer maximum is larger than the maxima of the overlying additional layers. Thus simultaneous observations of the ground-based  $F3$  layer and the topside ledge are required. A new topside sounding satellite with low orbit inclination is needed to accord with the increased new-built ionosondes at low latitudes. Also the future project of COSMIC II may also be helpful in clarifying the relationship between the  $F3$  layer and the topside ledge.

(3) Another important question concerns the mechanism of the  $F3$  layer formation. The main aspects of this issue are presented in Figure 22. Huang [15] found that the formation of daytime  $F2$  layer stratification is principally

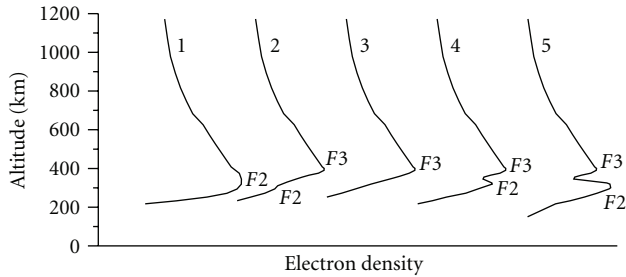


FIGURE 21: Sketch of diurnal variations of the electron density profile near the geomagnetic equator: (1) the daytime electron density profile with a one-layered pattern without  $F2$  layer stratifications. (2) the sunset electron density profile with a two-layered pattern—the  $F3$  layer appears due to the non-uniform in height vertical plasma drift and the  $F2$  layer disappears due to the reduction of photoionization, at that  $foF3 > foF2$ . (3) the nighttime electron density profile with a one-layered pattern—the  $F3$  layer occurs, the  $F2$  layer almost disappears. (4) the morning-noon electron density profile with a two-layered pattern—the  $F2$  layer appears due to the increase of photoionization and the  $F3$  layer continues to occur (this could also appear in the sunset local time). (5) the afternoon electron density profile with a two-layered pattern—the  $foF2$  continue increases due to the photoionization processes, at that  $foF3$  becomes smaller than  $foF2$ . Further the  $F3$  layer merges with  $F2$  layer, and the electron density profile turns type 1.

due to the combined effect of the upward drift, which changes from increasing to decreasing before noon, and the slow diffusion. Raghavarao and Sivaraman [67] suggested and Surotkin et al. [31] showed that the physical cause of the formation of  $F2$  layer stratifications is nonuniform diffusive plasma outflow from the region over the magnetic equator where the equatorial anomaly crests developed. Balan et al. [35] concluded that the  $F3$  layer is formed in the morning and daytime sector, when the ionization processes dominate over chemical losses due to upward plasma transport under the action of  $\mathbf{E} \times \mathbf{B}$  drift and neutral wind. Uemoto et al. [41] improve this mechanism by claiming that the field-aligned diffusion of plasma acts to make the  $F3$  layer prominent in the magnetic latitudes far off the magnetic equator region. Thampi et al. [54] proposed that an upward  $\mathbf{E} \times \mathbf{B}$  drift and strong equatorward neutral wind (perturbed by AGW) can produce the  $F3$  layer through the reduction in the downward diffusion of ionization along geomagnetic field lines. Klimentko et al. [46] and M. V. Klimentko and V. V. Klimentko [48] demonstrated that the  $F3$  layer is formed as a result of the non-uniform height vertical  $\mathbf{E} \times \mathbf{B}$  plasma drifts at the geomagnetic equator. The non-uniform height vertical  $\mathbf{E} \times \mathbf{B}$  plasma drifts leads to plasma convergence at some altitudes and to its rarefaction at others. So the mechanism of the  $F2$  layer stratification in the low latitudes is too complicated (see Figure 22), and we do not know which is dominant that well explained the observed phenomenon. Thus a detailed analysis is needed from a comprehensive study based on both the observation and modeling. In addition, using model studies, it is necessary to clarify the role of thermospheric tides and gravity waves

in the formation of additional layers in the low-latitude ionospheric  $F$  region.

(4) Also there is a question. What is the formation mechanism of the sunset and nighttime  $F3$  layer? Depuev and Pulinetz [51], Karpachev et al. [52], Zhao et al. [66] described the case of the  $F3$  layer occurrence at night (00:00–04:00 LT) and after sunset (18:00–21:00 LT). Klimentko et al. [46] and M. V. Klimentko and V. V. Klimentko [48] demonstrated that the non-uniformity in height vertical  $\mathbf{E} \times \mathbf{B}$  plasma drifts at the geomagnetic equator can explain the  $F3$  layer occurrence at different LT epochs (especially at night). The height gradients in vertical plasma drifts were previously observed by incoherent scatter radar over Jicamarca [75]. We need experimental verification of the hypothesis about the  $F3$  layer formation by non-uniformity in height  $\mathbf{E} \times \mathbf{B}$  plasma drifts. This verification will be based on the observational data of the electric field at different low latitudes or at different heights at the geomagnetic equator.

(5) Another interesting issue is the occurrence of the multilayer pattern in vertical profile of electron density. Sen [2] was the first to detect the presence of two additional peaks above regular  $F2$  layer in the ground-based ionograms over Singapore. Further no one mentioned the existence of multiple additional layers. M. V. Klimentko and V. V. Klimentko [47] demonstrated the occurrence of only one additional layer during solar activity minimum at quite equinox condition. Klimentko et al. [82] demonstrated the occurrence of several additional layers for quiet solstice conditions during solar activity maximum and Klimentko et al. [46] specified the formation of at least two additional layers above Jicamarca during geomagnetic storm event. Does the appearance of the multilayer pattern in electron density profile depend on season, geomagnetic and solar activity? We need more investigations on this issue. In addition, Surotkin et al. [31] showed that large-scale irregularities could decay into small-scale irregularities. Klimentko et al. [46] note that simultaneous occurrence of spread  $F$  in observational data and additional layers in model calculations do not contradict each other, as spread  $F$  and the formation of additional layers are related to the action of the same mechanism— $\mathbf{E} \times \mathbf{B}$  drift [15, 29, 35, 83]. M. V. Klimentko and V. V. Klimentko [48] showed the  $F3$  and  $F4$  layer occurrence at night when the spread  $F$  was usually observed. We need to find out the relationship between multiple  $F2$  layer stratifications and equatorial spread  $F$ .

(6) The next important aspect that needs further study on  $F3$  layer is the possible existence of the interrelationship between  $F3$  layer and other well-known features of the equatorial ionosphere. For example, a correlative study of the simultaneous occurrence of  $F3$  layer and CEJ [22] that requires the definite observational evidences of the causative mechanisms for the  $F3$  layer formation as well as for CEJ and their interrelation should be continued. Furthermore, the problem of the ledge ( $F3$  layer) location relative to the EIA crests and geomagnetic field lines cannot consider to be completely solved.

(7) Although the mechanism of the low-latitude  $F3$  layer during geomagnetic storm is mainly attributed to the PPEF, there are still unresolved problems. Lin et al. [58] proposed

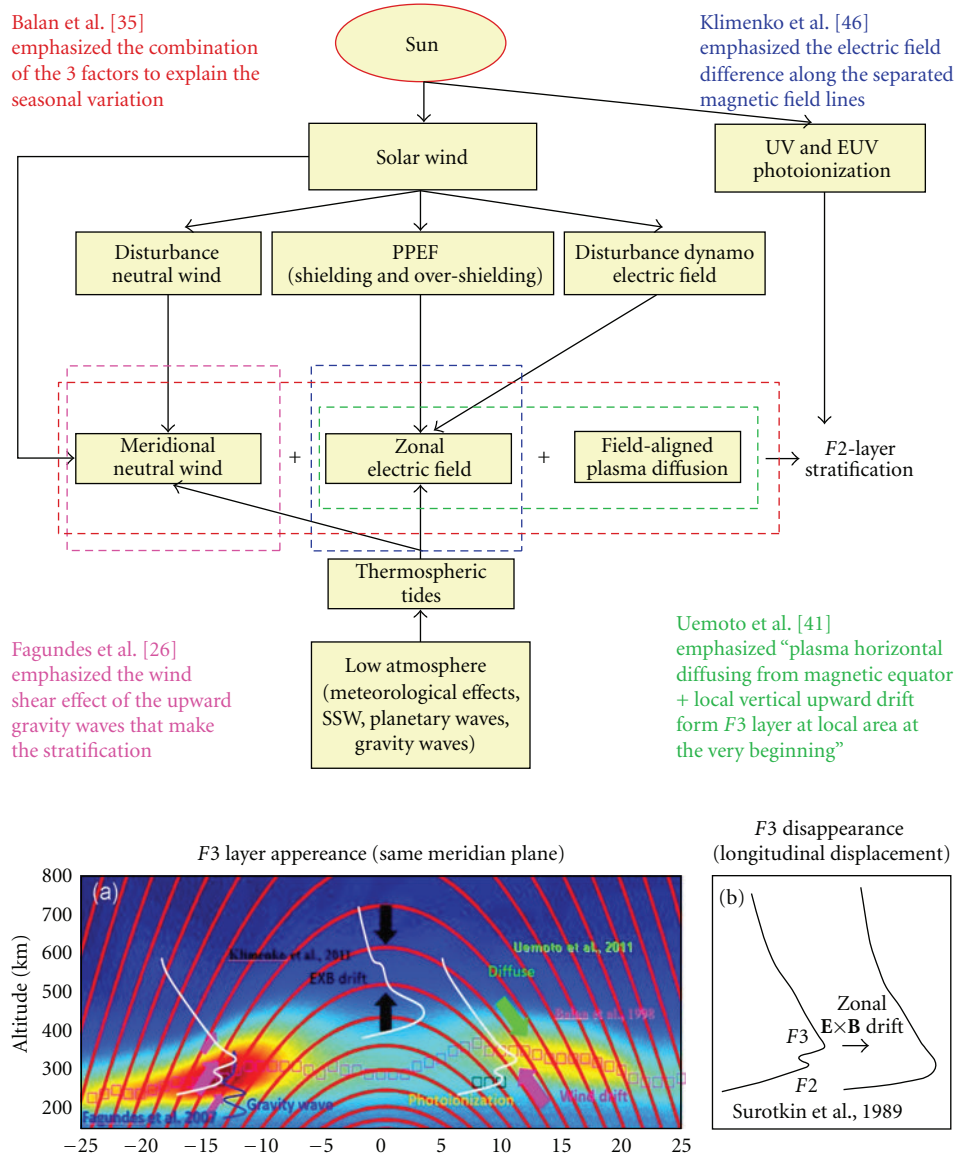


FIGURE 22: A schematic of the different mechanisms of the *F2* layer stratification and all influenced factors.

that the storm time wind surge may result in the nighttime *F2* stratification at low latitude; however, this mechanism needs observational proof. In addition, we do not know the effect of the disturbance dynamo electric field on the *F3* layer. Zhao et al. [84] showed that the normal daytime *F3* layer was inhibited during the recovery phase of a storm. Klimenko et al. [46] specified the formation of at least two additional layers above Jicamarca during geomagnetic storm event. Also the existing contradiction between the satellite and ground-based data on the occurrence probability of the *F3* layer during storm needs to be explored.

More ground observations needed to clarify the relationship between the every process in the lower atmosphere and the whole structure in the ionosphere (in particular *F3* layer), for example, the effect of the sudden stratospheric warming

(SSW) event on the ionosphere [85] that is recently being hotly investigated. Fortunately, in the future a number of new ionosondes will be installed and operated at the low and equatorial areas which may help to explain some of the puzzles or discrepancies in the past observations [86].

**Acknowledgments**

The authors thanks Drs. L.P. Goncharenko and K.G. Ratovsky for useful discussions. This research was supported by the National Natural Science Foundation of China (41174138), the National Important Basic Research Project (2011CB811405), and the Open Research Program of State Key Laboratory of Space Weather, Chinese Academy of

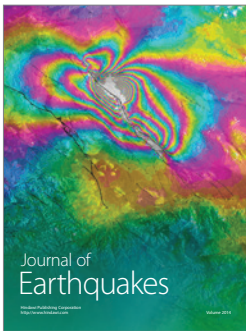
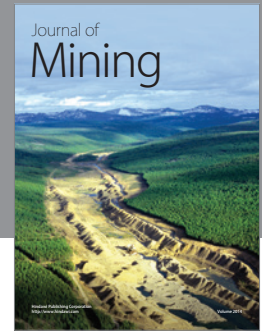
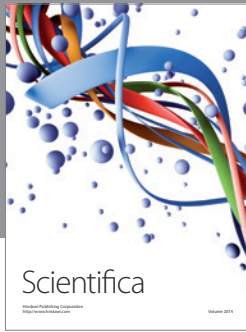
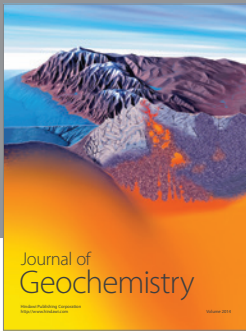
Sciences. Special thanks should be given to the Digisonde Global Ionospheric Radio Observatory (GIRO).

## References

- [1] D. K. Bailey, "The geomagnetic nature of the F2-layer longitude-effect," *Terrestrial Magnetism and Atmospheric Electricity*, vol. 53, no. 1, pp. 35–39, 1948.
- [2] H. Y. Sen, "Stratification of the F2 layer of the ionosphere over Singapore," *Journal of Geophysical Research*, vol. 54, p. 363, 1949.
- [3] B. W. Osborne, "Ionospheric behaviour in the F2 region at Singapore," *Journal of Atmospheric and Terrestrial Physics*, vol. 2, no. 1, pp. 66–78, 1951.
- [4] J. A. Ratcliffe, "Some regularities in the F2 region of the ionosphere," *Journal of Geophysical Research*, vol. 56, p. 487, 1951.
- [5] A. G. McNish, *Proceedings of the Conference on Ionospheric Physics, State College, Pennsylvania*, Section CC, 1950.
- [6] B. W. Osborne, "Lunar variations in F2 region critical frequency at Singapore," *Nature*, vol. 169, no. 4303, pp. 661–662, 1952.
- [7] N. J. Skinner, R. A. Brown, and R. W. Wright, "Multiple stratification of the F-layer at Ibadan," *Journal of Atmospheric and Terrestrial Physics*, vol. 5, no. 1–6, pp. 92–100, 1954.
- [8] L. H. Heisler, "The anomalous ionospheric stratification F1.5," *Journal of Atmospheric and Terrestrial Physics*, vol. 24, no. 6, pp. 483–489, 1962.
- [9] J. M. Faynot, P. Vila, and J. Walter, "Upward-moving irregularities in the subequatorial ionosphere," *Journal of Atmospheric and Terrestrial Physics*, vol. 33, no. 10, pp. 1621–1627, 1971.
- [10] R. G. Rastogi, "Upward moving irregularity (kink) in the equatorial ionosphere," *Annals of Geophysics*, vol. 29, no. 3, pp. 421–429, 1973.
- [11] T. Sario, M. Takeda, T. Araki et al., "A midday bite-out event of the F2-layer observed by MU radar," *Journal of Geomagnetism and Geoelectricity*, vol. 41, no. 8, pp. 727–734, 1989.
- [12] J. P. McClure and V. L. Peterson, "Plasma transport in the equatorial F region," *Radio Science*, vol. 7, no. 5, pp. 539–547, 1972.
- [13] R. F. Woodman, D. L. Sterling, and W. B. Hanson, "Synthesis of Jicamarca data during the great storm of March 8, 1970," *Radio Science*, vol. 7, pp. 739–746, 1972.
- [14] C. M. Huang, "Certain behavior of the ionospheric F2 region at low latitudes," *Radio Science*, vol. 9, no. 5, pp. 519–532, 1974.
- [15] C. M. Huang, "Travelling bifurcation of the equatorial F2 Layer," *Radio Science*, vol. 10, no. 5, pp. 507–516, 1975.
- [16] I. Iwamoto, "A study on the ion composition of the topside ionosphere by satellite-borne mass spectrometers," *Journal of the Communications Research Laboratory*, vol. 44, no. 1, pp. 11–186, 1997.
- [17] J. Sayers, P. Rothwell, and J. H. Wager, "Field aligned strata in the ionization above the ionospheric F2 layer," *Nature*, vol. 198, no. 4877, pp. 230–233, 1963.
- [18] G. E. K. Lockwood and G. L. Nelms, "Topside sounder observations of the equatorial anomaly in the 75° W longitude zone," *Journal of Atmospheric and Terrestrial Physics*, vol. 26, no. 5, p. 569, 1964.
- [19] J. W. King, P. A. Smith, D. Eceles, G. F. Fooks, and F. Helm, "Preliminary investigation of the structure of the upper ionosphere as observed by the topside sounder satellite Alouette 1," *Proceedings of the Royal Society*, vol. A281, no. 1389, p. 464, 1964.
- [20] R. Raghavarao and M. R. Sivaraman, "Ionisation ledges in the equatorial ionosphere," *Nature*, vol. 249, no. 5455, pp. 331–332, 1974.
- [21] R. Raghavarao, P. Sharma, and A. R. Jain, "Ionization ledges and the counter-electrojets in the equatorial ionosphere," *Space Research*, vol. 17, pp. 417–421, 1977.
- [22] P. Sharma and R. Raghavarao, "Simultaneous occurrence of ionization ledge and counter-electrojet in the equatorial ionosphere: observational evidence and its implications," *Canadian Journal of Physics*, vol. 67, no. 2-3, pp. 166–172, 1989.
- [23] I. S. Prutensky, "Stratification of the electron density in the topside low-latitude ionosphere from the Cosmos-1809 satellite data," *Geomagnetism and Aeronomy*, vol. 32, no. 5, pp. 99–103, 1992.
- [24] D. F. Martyn, "The morphology of the ionospheric variations associated with magnetic disturbance. I. variations at moderately low latitudes," *Proceedings of the Royal Society A*, vol. 218, no. 1132, pp. 1–18, 1953.
- [25] K. N. Vasiliev, "Geomagnetic effect in the vertical movements of ionization in the ionosphere F region," *Geomagnetism and Aeronomy*, vol. 7, no. 3, pp. 469–474, 1967 (Russian).
- [26] P. R. Fagundes, V. Klausner, Y. Sahai et al., "Observations of daytime F2-layer stratification under the southern crest of the equatorial ionization anomaly region," *Journal of Geophysical Research A*, vol. 112, no. 4, Article ID A04302, 2007.
- [27] D. N. Anderson, "A theoretical study of the ionospheric F region equatorial anomaly-I. Theory," *Planetary and Space Science*, vol. 21, no. 3, pp. 409–419, 1973.
- [28] V. A. Surotkin, O. P. Kolomijtsev, and A. A. Namgaladze, *Numerical Modelling of the F2-Region Stratifications at the Near-Equatorial Ionosphere, Ionosphere-Magnetospheric Disturbances and Its Predictions*, Nauka, Moscow, Russia, 1984.
- [29] V. A. Surotkin, A. A. Namgaladze, and O. P. Kolomijtsev, "Modelling of the diurnal development of the equatorial ionospheric F2-region bifurcations," *Geomagnetism and Aeronomy*, vol. 25, no. 3, pp. 394–399, 1985 (Russian).
- [30] N. M. Kashchenko and M. A. Nikitin, "Particularities of the formation of stratifications in the daytime equatorial F-region," *Geomagnetism and Aeronomy*, vol. 27, no. 3, pp. 501–504, 1987.
- [31] V. A. Surotkin, A. A. Namgaladze, and O. P. Kolomijtsev, "On the physical mechanism of formation of one type F2-region pattern splitting in the equatorial ionosphere," *Radiophysics*, vol. 32, no. 3, pp. 952–956, 1989 (Russian).
- [32] N. Balan and J. G. Bailey, "Equatorial plasma fountain and its effects: possibility of an additional layer," *Journal of Geophysical Research*, vol. 100, no. A11, p. 421, 1995.
- [33] N. Balan, G. J. Bailey, M. A. Abdu et al., "Equatorial plasma fountain and its effects over three locations: evidence for an additional layer, the F3 layer," *Journal of Geophysical Research A*, vol. 102, no. 2, Article ID 95JA02639, pp. 2047–2056, 1997.
- [34] B. Jenkins, G. J. Bailey, M. A. Abdu, I. S. Batista, and N. Balan, "Observations and model calculations of an additional layer in the topside ionosphere above Fortaleza, Brazil," *Annales Geophysicae*, vol. 15, no. 6, pp. 753–759, 1997.
- [35] N. Balan, I. S. Batista, M. A. Abdu, J. Macdougall, and G. J. Bailey, "Physical mechanism and statistics of occurrence of an additional layer in the equatorial ionosphere," *Journal of Geophysical Research*, vol. 103, pp. 169–181, 1998.
- [36] N. Balan, I. S. Batista, M. A. Abdu et al., "Variability of an additional layer in the equatorial ionosphere over Fortaleza," *Journal of Geophysical Research A*, vol. 105, no. 5, Article ID 1999JA000020, pp. 10603–10613, 2000.

- [37] C. C. Hsiao, J. Y. Liu, R. T. Tsunoda et al., "Evidence for the geographic control of additional layer formation in the low-latitude ionosphere," *Advances in Space Research*, vol. 27, no. 6-7, pp. 1293–1297, 2001.
- [38] I. S. Batista, M. A. Abdu, J. MacDougall, and J. R. Souza, "Long term trends in the frequency of occurrence of the F3 layer over Fortaleza, Brazil," *Journal of Atmospheric and Solar-Terrestrial Physics*, vol. 64, no. 12-14, pp. 1409–1412, 2002.
- [39] P. V. S. Rama Rao, K. Niranjana, D. S. V. V. D. Prasad, P. S. Brahmanandam, and S. Gopikrishna, "Features of additional stratification in ionospheric F2 layer observed for half a solar cycle over Indian low latitudes," *Journal of Geophysical Research A*, vol. 110, no. 4, Article ID A04307, 2005.
- [40] J. Uemoto, T. Ono, T. Maruyama, S. Saito, M. Iizima, and A. Kumamoto, "Magnetic conjugate observation of the F3 layer using the SEALION ionosonde network," *Geophysical Research Letters*, vol. 34, no. 2, Article ID L02110, 2007.
- [41] J. Uemoto, T. Maruyama, T. Ono, S. Saito, M. Iizima, and A. Kumamoto, "Observations and model calculations of the F3 layer in the Southeast Asian equatorial ionosphere," *Journal of Geophysical Research*, vol. 116, article A03311, 2011.
- [42] A. F. M. Zain, S. Abdullah, M. J. Homam, F. C. Seman, M. Abdullah, and Y. H. Ho, "Observations of the F3-layer at equatorial region during 2005," *Journal of Atmospheric and Solar-Terrestrial Physics*, vol. 70, no. 6, pp. 918–925, 2008.
- [43] V. Sreeja, S. Ravindran, and T. K. Pant, "Features of the F3 layer occurrence over the equatorial location of Trivandrum," *Annales Geophysicae*, vol. 28, no. 9, pp. 1741–1747, 2010.
- [44] N. Balan, I. S. Batista, M. A. Abdu, J. H. A. Sobral, J. MacDougall, and G. J. Bailey, "Occurrence of an additional layer in the ionosphere over Fortaleza," *Advances in Space Research*, vol. 24, no. 11, pp. 1481–1484, 1999.
- [45] M. V. Klimenko, V. V. Klimenko, K. G. Ratovsky, and L. P. Goncharenko, "Disturbances in the ionospheric F-region peak heights in the American longitudinal sector during geomagnetic storms of September 2005," *Advances in Space Research*, vol. 48, no. 7, pp. 1184–1195, 2011.
- [46] M. V. Klimenko, V. V. Klimenko, K. G. Ratovsky et al., "Numerical modeling of ionospheric effects in the middle- and low-latitude F region during geomagnetic storm sequence of 9–14 September 2005," *Radio Science*, vol. 46, no. 3, 2011.
- [47] M. V. Klimenko and V. V. Klimenko, "Numerical modeling of F2-layer stratification and occurrence of the F3- and G-layers in equatorial ionosphere—The event morphology," *Geomagnetism and Aeronomy*, vol. 51, no. 5, pp. 646–655, 2011.
- [48] M. V. Klimenko and V. V. Klimenko, "Mechanisms of F2-layer stratification and formation of the F3- and G-layers in the equatorial ionosphere," *Geomagnetism and Aeronomy*, vol. 52, no. 3, pp. 321–334, 2012.
- [49] J. Uemoto, T. Ono, A. Kumamoto, and M. Iizima, "Ionization ledge structures observed in the equatorial anomaly region by using PPS system on-board the Ohzora (EXOS-C) satellite," *Earth, Planets and Space*, vol. 56, no. 7, pp. e21–e24, 2004.
- [50] J. Uemoto, T. Ono, A. Kumamoto, and M. Iizima, "Statistical analysis of the ionization ledge in the equatorial ionosphere observed from topside sounder satellites," *Journal of Atmospheric and Solar-Terrestrial Physics*, vol. 68, no. 12, pp. 1340–1351, 2006.
- [51] V. H. Depuev and S. A. Pulnits, "Intercosmos-19 observations of an additional topside ionization layer: the F3 layer," *Advances in Space Research*, vol. 27, no. 6-7, pp. 1289–1292, 2001.
- [52] A. T. Karpachev, M. V. Klimenko, V. V. Klimenko, G. A. Zbankov, and V. A. Telegin, "Latitudinal structure of the equatorial F3 layer on the basis of the Intercosmos-19 topside sounding data," *Journal of Atmospheric and Solar-Terrestrial Physics*, vol. 77, pp. 186–193, 2012.
- [53] S. V. Thampi, S. Ravindran, C. V. Devasia, T. K. Pant, P. Sreelatha, and R. Sridharan, "First observation of topside ionization ledges using radio beacon measurements from low Earth orbiting satellites," *Geophysical Research Letters*, vol. 32, no. 11, pp. 1–4, 2005.
- [54] S. V. Thampi, N. Balan, S. Ravindran et al., "An additional layer in the low-latitude ionosphere in Indian longitudes: total electron content observations and modeling," *Journal of Geophysical Research A*, vol. 112, no. 6, Article ID A06301, 2007.
- [55] B. Zhao, W. Wan, X. Yue et al., "Global characteristics of occurrence of an additional layer in the ionosphere observed by COSMIC/FORMOSAT F3," *Geophysical Research Letters*, vol. 38, article L02101, 2011.
- [56] N. Balan, S. V. Thampi, K. Lynn et al., "F3 layer during penetration electric field," *Journal of Geophysical Research A*, vol. 113, no. 3, Article ID A00A07, 2008.
- [57] V. Sreeja, N. Balan, R. Sudha, T. K. Pant, R. Sridharan, and G. J. Bailey, "Additional stratifications in the equatorial F region at dawn and dusk during geomagnetic storms: role of electrodynamics," *Journal of Geophysical Research A*, vol. 114, no. 8, Article ID A08309, 2009.
- [58] C. H. Lin, A. D. Richmond, G. J. Bailey, J. Y. Liu, G. Lu, and R. A. Heelis, "Neutral wind effect in producing a storm time ionospheric additional layer in the equatorial ionization anomaly region," *Journal of Geophysical Research A*, vol. 114, no. 9, 2009.
- [59] C. H. Lin, A. D. Richmond, J. Y. Liu, G. J. Bailey, and B. W. Reinisch, "Theoretical study of new plasma structures in the low-latitude ionosphere during a major magnetic storm," *Journal of Geophysical Research A*, vol. 114, no. 5, 2009.
- [60] R. G. Roble, E. C. Ridley, A. D. Richmond, and R. E. Dickinson, "A coupled thermosphere/ionosphere general circulation model," *Geophysical Research Letters*, vol. 15, pp. 1325–1328, 1988 ..
- [61] A. D. Richmond, E. C. Ridley, and R. G. Roble, "A thermosphere/ionosphere general circulation model with coupled electrodynamics," *Geophysical Research Letters*, vol. 19, no. 6, pp. 601–604, 1992.
- [62] A. A. Namgaladze, Y. N. Korenkov, V. V. Klimenko et al., "Global model of the thermosphere-ionosphere-protonosphere system," *Pure and Applied Geophysics*, vol. 127, no. 2-3, pp. 219–254, 1988.
- [63] M. V. Klimenko, V. V. Klimenko, and V. V. Bryukhanov, "Numerical simulation of the electric field and zonal current in the Earth's ionosphere: the dynamo field and equatorial electrojet," *Geomagnetism and Aeronomy*, vol. 46, no. 4, pp. 457–466, 2006.
- [64] J. D. Huba, G. Joyce, and J. A. Fedder, "Sami2 is Another Model of the Ionosphere (SAMI2): a new low-latitude ionosphere model," *Journal of Geophysical Research A*, vol. 105, no. 10, Article ID 2000JA000035, pp. 23035–23053, 2000.
- [65] K. J. W. Lynn, T. J. Harris, and M. Sjarifudin, "Stratification of the F2 layer observed in Southeast Asia," *Journal of Geophysical Research A*, vol. 105, no. 12, Article ID 2000JA900056, pp. 27147–27156, 2000.
- [66] B. Zhao, W. Wan, B. Reinisch et al., "Features of the F3 layer in the low-latitude ionosphere at sunset," *J. Geophys. Res.*, vol. 116, article A01313, 2011.

- [67] R. Raghavarao and M. R. Sivaraman, "Ionization ledges in the equatorial ionosphere," *Nature*, vol. 15, pp. 385–391, 1975.
- [68] B. G. Fejer, J. W. Jensen, and S. Y. Su, "Quiet time equatorial F region vertical plasma drift model derived from ROCSAT-1 observations," *Journal of Geophysical Research A*, vol. 113, no. 5, Article ID A05304, 2008.
- [69] N. A. Kochenova, "Longitudinal variations of the equatorial ionosphere according to Intercosmos-19 data," *Geomagnetism and Aeronomy*, vol. 21, no. 1, pp. 142–144, 1987.
- [70] A. T. Karpachev, "Characteristics of the global longitudinal effect in the night-time equatorial anomaly," *Geomagnetism and Aeronomy*, vol. 28, no. 1, pp. 46–49, 1988.
- [71] G. F. Deminova, "Fine structure of foF2 longitudinal distribution in the night-time low-latitude ionosphere derived from Intercosmos-19 topside sounding data," *Advances in Space Research*, vol. 31, no. 3, pp. 531–536, 2003.
- [72] H. Kil, E. R. Talaat, S. J. Oh, L. J. Paxton, S. L. England, and S. Y. Su, "Wave structures of the plasma density and vertical  $E \times B$  drift in low-latitude F region," *Journal of Geophysical Research A*, vol. 113, no. 9, Article ID A09312, 2008.
- [73] J. Oberheide, J. M. Forbes, X. Zhang, and S. L. Bruinsma, "Wave-driven variability in the ionosphere-thermosphere-mesosphere system from TIMED observations: what contributes to the "wave 4"?" *Journal of Geophysical Research*, vol. 116, Article ID A01306, 15 pages, 2011.
- [74] B. G. Fejer, E. R. de Paula, S. A. Gonzales, and R. F. Woodman, "Average vertical and zonal F region plasma drifts over Jicamarca," *Journal of Geophysical Research*, vol. 96, pp. 13,901–13,906, 1991.
- [75] J. E. Pingree and B. G. Fejer, "On the height variation of the equatorial F region vertical plasma drifts," *Journal of Geophysical Research*, vol. 92, no. A5, pp. 4763–4766, 1987.
- [76] B. Zhao, W. Wan, and L. Liu, "Responses of equatorial anomaly to the October-November 2003 superstorms," *Annales Geophysicae*, vol. 23, no. 3, pp. 693–706, 2005.
- [77] V. V. Paznukhov, B. W. Reinisch, P. Song, X. Huang, T. W. Bullett, and O. Veliz, "Formation of an F3 layer in the equatorial ionosphere: a result from strong IMF changes," *Journal of Atmospheric and Solar-Terrestrial Physics*, vol. 69, no. 10-11, pp. 1292–1304, 2007.
- [78] N. Balan, M. Yamamoto, V. Sreeja et al., "A statistical study of the response of the dayside equatorial F2 layer to the main phase of intense geomagnetic storms as an indicator of penetration electric field," *Journal of Geophysical Research*, vol. 116, Article ID A03323, 15 pages, 2011.
- [79] P. R. Fagundes, V. Klausner, J. A. Bittencourt, Y. Sahai, and J. R. Abalde, "Seasonal and solar cycle dependence of F3-layer near the southern crest of the equatorial ionospheric anomaly," *Advances in Space Research*, vol. 48, no. 3, pp. 472–477, 2011.
- [80] M. A. Abdu, I. S. Batista, I. J. Kantor, and J. H. A. Sobral, "Gravity wave induced ionization layers in the night F-region over Cachoeira Paulista (22°, 45°W)," *Journal of Atmospheric and Terrestrial Physics*, vol. 44, no. 9, pp. 759–767, 1982.
- [81] J. M. Forbes, "Planetary waves in the thermosphere-ionosphere system," *Journal of Geomagnetism and Geoelectricity*, vol. 48, no. 1, pp. 91–98, 1996.
- [82] M. V. Klimenko, V. V. Klimenko, and A. T. Karpachev, "Formation mechanism of additional layers above regular F2 layer in the near-equatorial ionosphere during quiet period," *Journal of Atmospheric and Solar-Terrestrial Physics*. In press.
- [83] M. A. Abdu, "Outstanding problems in the equatorial ionosphere-thermosphere electrodynamics relevant to spread F," *Journal of Atmospheric and Solar-Terrestrial Physics*, vol. 63, no. 9, pp. 869–884, 2001.
- [84] B. Zhao, W. Wan, L. Liu, K. Igarashi, K. Yumoto, and B. Ning, "Ionospheric response to the geomagnetic storm on 13-17 April 2006 in the West Pacific region," *Journal of Atmospheric and Solar-Terrestrial Physics*, vol. 71, no. 1, pp. 88–100, 2009.
- [85] L. P. Goncharenko, A. J. Coster, J. L. Chau, and C. E. Valladares, "Impact of sudden stratospheric warmings on equatorial ionization anomaly," *Journal of Geophysical Research A*, vol. 115, no. 10, Article ID A00G07, 2010.
- [86] B. W. Reinisch and I. A. Galkin, "Global ionospheric radio observatory (GIRO)," *Earth Planets Space*, vol. 63, pp. 377–381, 2011.



**Hindawi**

Submit your manuscripts at  
<http://www.hindawi.com>

